1

The Changing El Niño–Southern Oscillation and Associated Climate Extremes

Jin-Yi Yu[1], Xin Wang[2], Song Yang[3,4], Houk Paek[1], and Mengyan Chen[2]

ABSTRACT

The El Niño–Southern Oscillation (ENSO) is one of the most powerful climate phenomena that produce profound global impacts. Extensive research since the 1970s has resulted in a theoretical framework capable of explaining the observed properties and impacts of the ENSO and predictive models. However, during the most recent two decades there have been significant changes observed in the properties of ENSO that suggest revisions are required in the existing theoretical framework developed primarily for the canonical ENSO. The observed changes include a shift in the location of maximum sea surface temperature variability, an increased importance in the underlying dynamics of coupled ocean-atmosphere process in the subtropical Pacific, and different remote atmospheric teleconnection patterns that give rise to distinct climate extremes. The causes of these recent changes in ENSO are still a matter of debate but have been attributed to both global warming and natural climate variability involving interactions between the Pacific and Atlantic oceans. The possible future changes of ENSO properties have also been suggested using climate model projections.

1.1. INTRODUCTION

El Niño–Southern Oscillation (ENSO) is a prominent climate phenomenon in the tropical Pacific that can disrupt global atmospheric and oceanic circulation patterns and exert profound impacts on global climate and socioeconomic activities. Since *Bjerknes* [1969] first recognized that ocean-atmosphere coupling was a fundamental characteristic of ENSO, a tremendous amount of effort has been expended by the research community to describe and understand the complex nature of this phenomenon and its underlying generation mechanisms. By the 1990s, the effort had led to the developments of successful theoretical frameworks that could explain the major features observed during ENSO events [*Neelin et al.*, 1998] and useful forecast systems had been formulated to predict ENSO evolution with significant lead times of up to three seasons [*Latif et al.*, 1998]. The typical ENSO impacts in various parts of the globe had also been extensively examined and documented. Through these efforts, it was also recognized that ENSO properties were not the same among events and could change from one decade to another. The diversity of ENSO characteristics attracted renewed interest at the beginning of the 21st century (see *Capotondi et al.* [2015], for a summary of these efforts), when it became obvious that the central location of the

[1] *Department of Earth System Science, University of California, Irvine, California, USA*

[2] *State Key Laboratory of Tropical Oceanography, South China Sea Institute of Oceanology, Chinese Academy of Sciences, Guangzhou, Guangdong, China*

[3] *School of Atmospheric Sciences, Sun Yat-sen University, GuangZhou, Guangdong, China*

[4] *Guangdong Province Key Laboratory for Climate Change and Natural Disaster Studies*

Climate Extremes: Patterns and Mechanisms, Geophysical Monograph 226, First Edition.
Edited by S.-Y. Simon Wang, Jin-Ho Yoon, Christopher C. Funk, and Robert R. Gillies.

sea surface temperature (SST) anomalies associated with ENSO appeared to be moving from the tropical eastern Pacific near the South American coast to locations near the International Dateline in the tropical central Pacific. Most of the El Niño events that have occurred so far in the 21st century developed primarily in the central Pacific [*Lee and McPhaden*, 2010; *Yu et al.*, 2012b; *Yu et al.*, 2015a; *Yeh et al.*, 2015]. The fact that El Niño can sometimes occur in the eastern Pacific, sometimes in the central Pacific, and sometimes simultaneously in both portions of the Pacific has suggested that there may exist more than one type of ENSO, whose generation mechanisms and associated climate extremes may be different. The changes in ENSO observed during the recent decades have motivated the research community to revisit the conventional views of ENSO properties, dynamics, and global impacts.

1.2. CHANGES IN ENSO PROPERTIES

1.2.1. Flavors of ENSO

Slow or interdecadal changes have been observed in ENSO properties, including its intensity, period, and propagation direction [*Gu and Philander*, 1995; *Wang and Wang,* 1996; *Torrence and Webster*, 1999; *An and Wang*, 2000; *Fedorov and Philander*, 2000; *Wang and An*, 2001; *Timmermann*, 2003; *An and Jin*, 2004; and many others]. The amplitude of ENSO-associated SST anomalies, for example, was found to be stronger at the beginning and the end of the twentieth century, but weaker in between [*Gu and Philander*, 1995; *Wang and Wang*, 1996]. The propagation direction of ENSO SST anomalies has also alternated between eastward, westward, and standing during the past few decades [*Wang and An*, 2001; *An and Jin*, 2004]. Its recurrence frequency changed from about 2 to 3 yr before 1975 to a longer frequency of 4 to 6 yr afterward [*An and Wang*, 2000]. In recent decades, one of the most noticeable changes in ENSO properties has been the displacement of the central location of ENSO SST anomalies [*Larkin and Harrison*, 2005; *Ashok et al.,* 2007; *Kao and Yu,* 2009; *Kug et al.,* 2009]. ENSO is characterized by interannual SST variations in the equatorial eastern and central Pacific. In the canonical ENSO events portrayed by *Rasmusson and Carpenter* [1982], SST anomalies first occur near the South American coast and then spread westward along the equator. However, ENSO events characterized by SST anomalies primarily in the equatorial central Pacific, and which spread eastward [*An and Wang*, 2000] also occur. *Trenberth and Stepaniak* [2001] recognized that the different SST evolutions of ENSO events cannot be fully described with a single index such as the Niño-3 (5°S–5°N, 90°–150°W) SST index. They defined a trans-Niño index, which measures the SST gradient along the equator by taking the difference between normalized Niño-1 + 2 (10°S–0°, 80°–90°W) and Niño-4 (5°S–5°N, 160°E–150°W) SST indices to help discriminate the different SST evolutions. Their study implies that different types of ENSO may be better identified by contrasting SST anomalies between the eastern and central Pacific. A similar conclusion was reached by *Yu and Kao* [2007] in their analysis of the persistence barrier of Niño indices in the central-to-eastern Pacific (i.e., Niño-1 + 2, Niño-3, Niño-3.4 (5°S–5°N, 120°–170°W), and Niño-4 SST indices). They found different decadal changes between the indices in the equatorial central and eastern Pacific. They also found that the decadal changes in ocean heat content variations along the equatorial Pacific coincide with the decadal changes in the SST persistence barriers in the eastern Pacific, but not with those in the central Pacific. This finding led them to suggest that there are two types of ENSO: An Eastern-Pacific (EP) type located primarily in the tropical eastern Pacific and whose generation mechanism involves equatorial thermocline variations, and a Central-Pacific (CP) type located in the central tropical Pacific and whose generation is less sensitive to thermocline variations. A detailed comparison of these two types of ENSO was presented in *Kao and Yu* [2009], where they identified the spatial structure, temporal evolution, and underlying dynamics of these two types of events. While this "two types of ENSO" point of view is adopted in this chapter, it should be noted that debate remains (for example, see the discussion in *Capotondi et al.* [2015]) as to whether these two types are really dynamically distinct.

Examples of the EP and CP types of ENSO are shown in Figure 1.1, which displays the SST anomaly patterns during the peak phase of the 1977–1978 and 1997–1998 El Niño events. During the 1997–1998 El Niño (Fig. 1.1a), SST anomalies were mostly located in the eastern part of the tropical Pacific, extending from the South American coast around 80°W to 160°W, covering the Niño-1 + 2 and Niño-3 regions. During the 1977–1978 El Niño (Fig. 1.1b), SST anomalies were mostly concentrated in the equatorial central Pacific from 160°E to 120°W, covering the Niño-3.4 and Niño-4 regions. Some early studies had already noticed the existence of a group of ENSO events that developed in the central Pacific around the International Dateline [e.g., *Weare et al.,* 1976; *Fu et al.,* 1986; *Hoerling and Kumar,* 2002; *Larkin and Harrison,* 2005a]. *Larkin and Harrison* [2005a] suggested that this group of ENSO events can produce different impacts on the US climate from conventional ENSO events and referred to them as the Dateline El Niño. *Ashok et al.* [2007] also focused on this group of ENSO events and termed them El Niño Modoki. Furthermore, *Wang and Wang* [2013] classified El Niño Modoki into two subtypes: El Niño Modoki I and El Niño Modoki II because

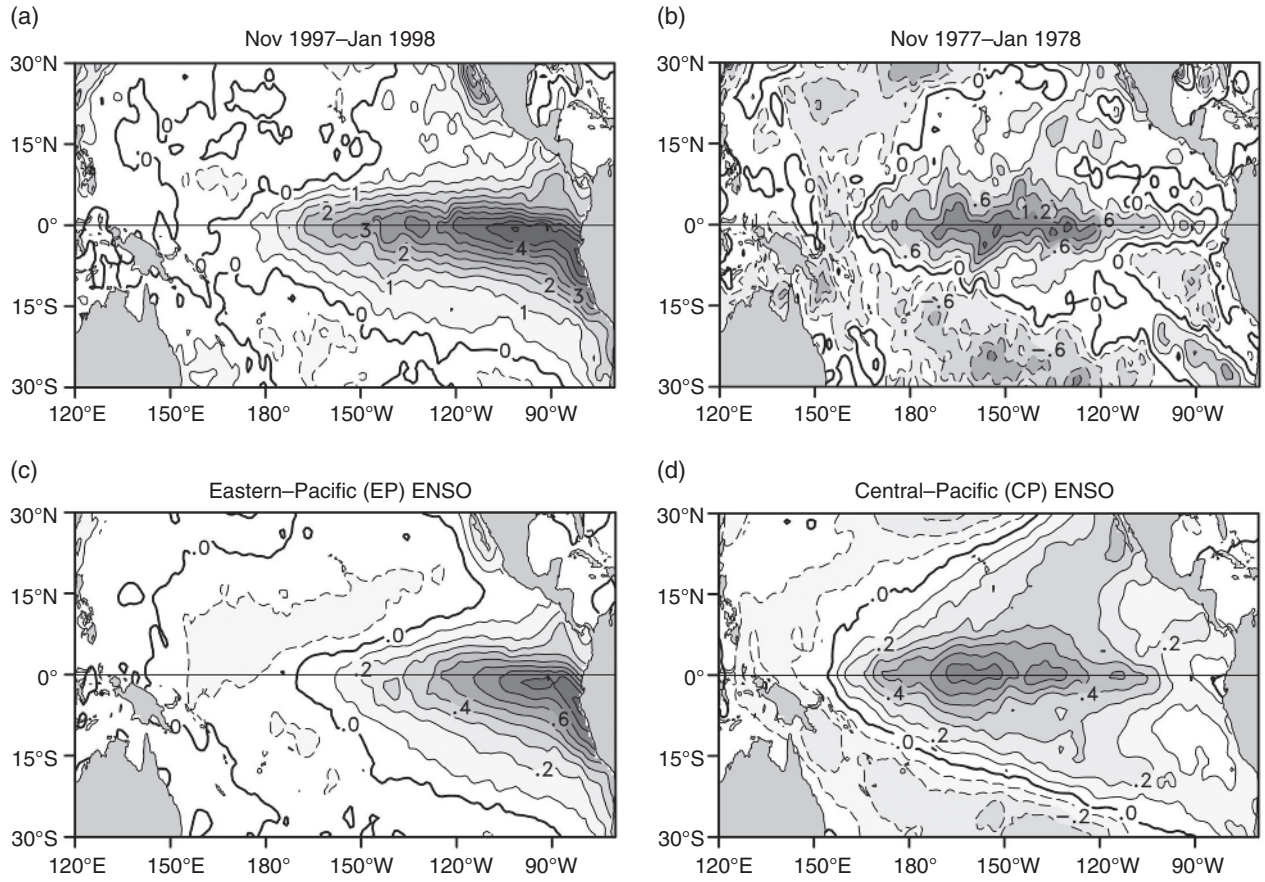

Figure 1.1 SST anomalies during the peak phase (November–January) of (a) the 1997–1998 El Niño event and (b) the 1977–1978 El Niño event. The leading EOF (empirical orthogonal function) patterns obtained from a regression-EOF analysis [*Kao and Yu*, 2009] are shown in (c) for the Eastern-Pacific type of ENSO and in (d) for the Central-Pacific type of ENSO. The contour intervals are 0.5 °C for (a), 0.3 °C for (b), and 0.1 °C for (c) and (d). The Hadley Centre Sea Ice and Sea Surface Temperature dataset (HadISST) [*Rayner et al.,* 2003] for the period 1948–2010 is used in these calculations.

they show significantly different impacts on rainfall in southern China and typhoon landfall activity. These two subtypes of El Niño Modoki have distinct origins and patterns of SST anomalies during their developing phase. *Kug et al.* [2009] also named this ENSO-type warm pool El Niño and the other type cold tongue El Niño.

1.2.2. Distinct Characteristics of the Eastern-Pacific (EP) and Central-Pacific (CP) Types of ENSO

Significant differences were found between the structure and evolution of the EP and CP types of ENSO [*Kao and Yu,* 2009; *Kug et al.,* 2009]. The typical SST anomaly patterns associated with these two types of ENSO are shown in Figure 1.1c and d, which are obtained by applying a regression-EOF (empirical orthogonal function) analysis [*Kao and Yu,*2009; *Yu and Kim*, 2010a] to tropical Pacific SST anomalies. In this method, SST anomalies regressed on the Niño-1 + 2 SST index (representing the EP ENSO influence) were first removed from the original monthly SST anomalies, and then an EOF analysis was applied to the residual SST anomalies to obtain the spatial pattern of the CP ENSO. Similarly, SST anomalies regressed on the Niño-4 index (representing the CP ENSO influence) were first removed from the original SST anomalies, and then an EOF analysis was applied to identify the leading structure of the EP ENSO. The principal components (PCs) associated with these patterns are referred to, respectively, as the CP ENSO index and the EP ENSO index. The EOF patterns show that the EP ENSO-related SST anomalies are mostly located in the eastern equatorial Pacific and connected to the coast of South America (Fig. 1.1c), while the CP ENSO has most of its SST anomalies confined in the central Pacific with extension into the northeastern subtropical Pacific (Fig. 1.1d). Although other studies also proposed different identification methodologies for separating the two types of ENSO, including weighted averaged SST

anomalies in the tropical western, central, and eastern Pacific [*Ashok et al.,* 2007]; relative magnitudes of the Niño-3 and Niño-4 indices [*Kug et al.,* 2009; *Yeh et al.,* 2009]; a simple transformation of the Niño-3 and Niño-4 indices [*Ren and Jin,* 2011] or two PCs of tropical Pacific SST anomalies [*Takahashi et al.,* 2011]; and mean upper ocean temperature anomalies in CP and EP regions [*Yu et al.,* 2011], their corresponding SST anomaly patterns are similar to those shown in Figure 1.1c and d. The SST anomaly features revealed by the regression-EOF analysis were observed in the 1977–1978 and 1997–1998 El Niño events as shown in Figure 1.1a and b. The meridional extension into the subtropics of the CP ENSO SST anomalies is an important feature, because it resembles the Pacific Meridional Mode (PMM) [*Chiang and Vimont,* 2004] that is the leading coupled variability mode of the subtropical Pacific. This connection indicates that the CP ENSO dynamic has a stronger tie to atmospheric and oceanic process outside the tropical Pacific than does the EP ENSO dynamic.

Below the ocean surface (Fig. 1.2), the EP ENSO is accompanied by significant subsurface temperature anomalies propagating across the Pacific basin, while the CP ENSO is associated only with subsurface ocean temperature anomalies that develop in situ in the central Pacific. The different subsurface evolution indicates that, in contrast to the EP ENSO, the underlying dynamics of the CP ENSO seem to be less dependent on thermocline variations [*Kao and Yu,* 2009; *Kug et al.,* 2009], which is consistent with the suggestion of *Yu and Kao* [2007]. *McPhaden* [2008] already noticed that the variations in the equatorial Pacific Ocean heat content (i.e., the so-called warm water volume; *Meinen and McPhaden* [2000]) tended to lead the ENSO SST anomalies by about two to three seasons in the 1980s and 1990s but by only one season after 2000. *McPhaden* [2012] attributed this decrease to the shift of ENSO from the EP type to the CP type in recent decades. The decreased lead time implies a reduced impact of thermocline feedback to SST anomalies for the CP ENSO and may explain the reduced predictability observed in recent decades [*Barnston et al.,* 2012] as this type of ENSO occurred more frequently. The weakened relationship between ENSO SST anomalies and the underlying thermocline variation indicates that the CP ENSO dynamic differs from the traditional ENSO dynamic, such as the delayed oscillator theory [*Suarez and Schopf,* 1988; *Battisti and Hirst,* 1989] or the recharged oscillator theory [e.g., *Wyrtki* 1975; *Zebiak* 1989; *Jin* 1997] that emphasize the subsurface ocean dynamics in governing ENSO SST evolution.

In the atmosphere, wind stress and precipitation anomaly patterns associated with the two types of ENSO are also different. While the EP El Niño is associated with significant westerly anomalies over a large part of the tropical Pacific, the westerly anomalies associated with the CP El Niño have a smaller spatial scale and are centered in the equatorial central-to-western Pacific [*Kao and Yu,* 2009; *Kug et al.,* 2009]. This more westward location of the westerly anomalies in the CP El Niño is consistent with the location of its SST anomalies. Significant easterly anomalies also appear over the tropical eastern Pacific during the CP El Niño. Theses anomalies were suggested to prevent the development of positive SST anomalies in this region during CP El Niño events [*Ashok et al.,* 2007; *Kug et al.,* 2009]. These differences in wind stress anomalies are important to the interpretation of the underlying dynamics of these two types of ENSO. Moreover, positive anomalies of precipitation associated with the EP El Niño typically extend from the equatorial eastern-to-central Pacific where the largest SST anomalies are located. For the CP El Niño, the precipitation anomalies are characterized by a dipole pattern, with positive anomalies located mainly in the western Pacific and negative anomalies in the eastern Pacific [*Kao and Yu,* 2009; *Kug et al.,* 2009]. The different precipitation patterns associated with these two types of ENSO imply that the locations of associated convective heating and the induced global teleconnections are different as well.

In addition to the central locations of their SST anomalies, the two types of ENSO also differ in their evolution, amplitude, and recurrence frequency. The propagation of SST anomalies is weaker and less apparent in the CP type of ENSO than in the EP type of ENSO [*Kao and Yu,* 2009]. Also, there is no identifiable phase-reversal signal in the composite analysis of the CP ENSO SST anomalies, implying that this type of ENSO does not behave like a cycle or oscillation as is often the case for the EP ENSO. Discussions of whether ENSO should be viewed as an event or a cycle [e.g., *Kessler,* 2002] might be aided by recognizing that there are two types of ENSO: one behaves more as an event and the other more as a cycle. *Sun and Yu* [2009] pointed out that the amplitude of the CP El Niño tends to be smaller than that of the EP El Niño, while the CP La Niña is often stronger than the EP La Niña. The reason for this difference in behavior between the El Niño and La Niña phases of these two types of ENSO has yet to be explained. *Sun and Yu* [2009], however, proposed an ENSO-mean state interaction mechanism to suggest that the amplitude asymmetries between the El Niño and La Niña phases of these two types of ENSO enable ENSO to modify the tropical Pacific mean state, which can give rise to a 10–15 yr modulation cycle in ENSO amplitude. Strong El Niño events can occur every 10–15 yr due to this cycle, which is consistent with the time interval between the last three strongest El Niño events: the 1972–1973, 1982–1983, and 1997–1998 El Niño events. For the recurrence frequency, it is well known that ENSO events tend to occur every 2

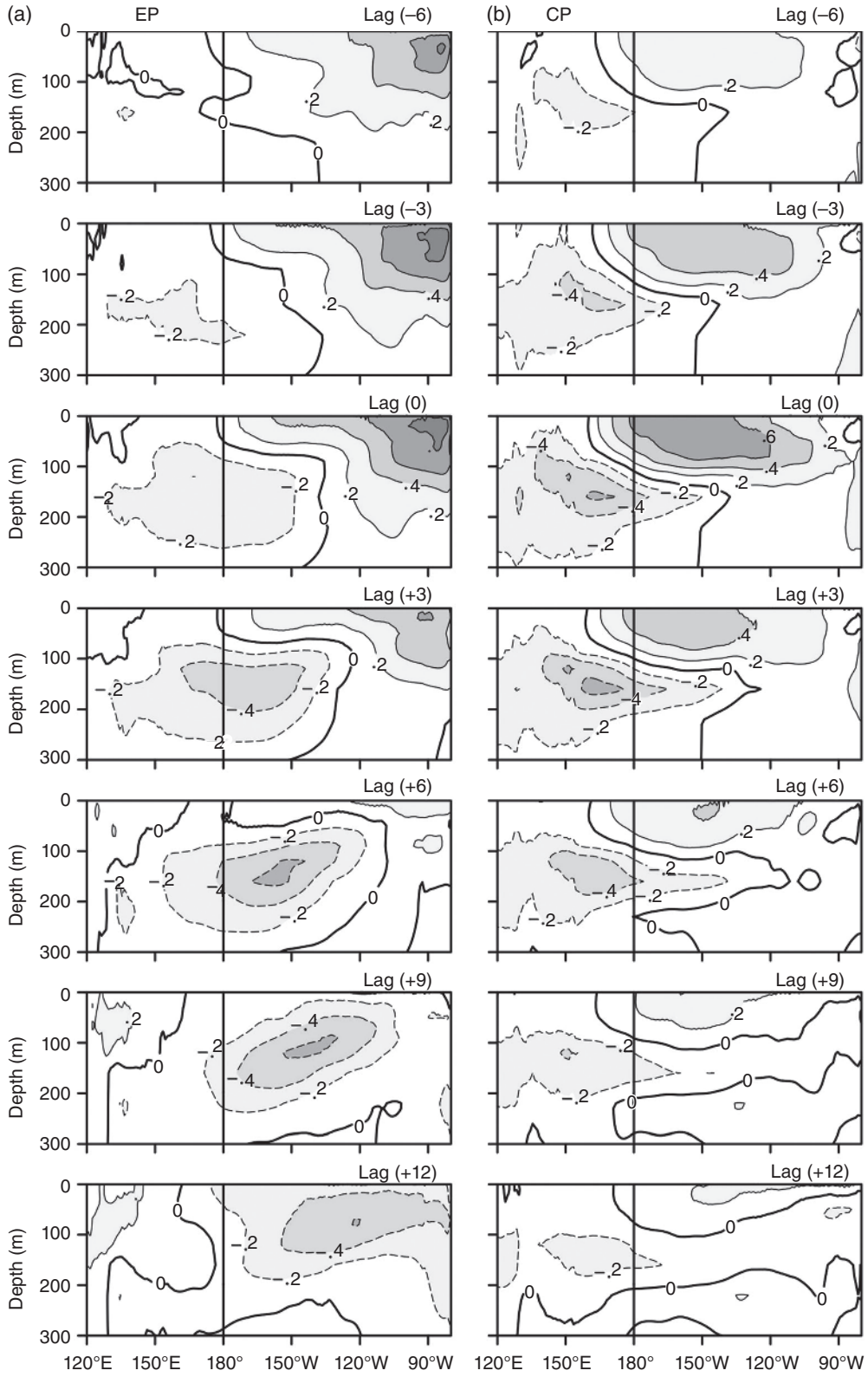

Figure 1.2 Evolution of equatorial (5°S–5°N) subsurface ocean temperature anomalies associated with the (a) EP ENSO and (b) CP ENSO. Values shown are temperature anomalies regressed on the EP and CP ENSO indices from a lag of –6 mo to a lag of +12 mo. The contour interval is 0.2 °C. Ocean temperature assimilation from the German Estimating the Circulation and Climate of the Ocean (GECCO) [*Kohl et al.,* 2006] for the period 1970–2001 is used.

to 7 yr. Spectral analyses have suggested that there are two dominant bands of ENSO variability: a quasibiennial (~2 yr) band and a low-frequency (3–7 yr) band [*Rasmusson and Carpenter,* 1982; *Rasmusson et al.,* 1990; *Barnett*, 1991; *Gu and Philander,* 1995; *Jiang et al.,* 1995; *Wang and Wang,* 1996]. The EP ENSO is dominated more by the low-frequency band, while the CP ENSO is dominated by the quasibiennial band [*Kao and Yu,* 2009; *Yu et al.,* 2010; *Yu and Kim*, 2010a]. As indicated above, El Niño events in the 21st century have been mostly of the CP type, and it is interesting to note that they occurred about every 2 yr in 2002, 2004, 2006, and 2009. In contrast, the El Niño events observed during the 1970s and 1980s tended to occur every 4 yr. If model projections are correct about the more frequent occurrence of the CP ENSO in the future warmer world [*Yeh et al.,* 2009; *Kim and Yu,* 2012], we should expect El Niño events in the coming decades to become more frequent but weaker.

1.2.3. Possible Causes for the Change in ENSO Properties

The recent change in the ENSO type may be due to background state changes in the tropical Pacific that are either caused by anthropogenic warming [*Yeh et al.,* 2009; *Kim and Yu*, 2012] or decadal/multidecadal natural variability [*McPhaden et al*., 2011; *Yeh et al.,* 2011]. Random fluctuations have also been suggested as possibly giving rise to the change in ENSO type on decadal timescales even without a change in the background state of the tropical Pacific [*Newman et al.,* 2011].

1.2.3.1. Anthropogenic Warming. *Yeh et al.* [2009] and *Kim and Yu* [2012] used multiple model datasets of phases 3 and 5 of the Coupled Model Intercomparison Project (CMIP3 and CMIP5) [*Meehl et al.,* 2007; *Taylor et al.,* 2012] to examine the influence of anthropogenic warming on the ENSO type. *Yeh et al.* [2009] analyzed CMIP3 model projections to show that anthropogenic warming can flatten the equatorial Pacific thermocline (due to a weakened Walker circulation) resulting in a shift of the thermocline feedback mechanism from eastern to central Pacific and increasing the occurrence of ENSO in the central Pacific. They suggested that the same mechanism may be at work in recent decades to increase the occurrence frequency of the CP ENSO. *Kim and Yu* [2012] compared the amplitude ratio of these two types of ENSO in CMIP5 models. They found that the intensity of the CP ENSO increases steadily from the preindustrial to the historical simulations and the future projections, but the intensity of the EP ENSO decreases. The CP-to-EP ENSO intensity ratio, as a result, is projected to increase.

This global warming view has been challenged on two fronts. First, *Lee and McPhaden* [2010] found that not only has the occurrence of the CP El Niño increased in recent decades but its intensity has also significantly increased. However, the intensity of CP La Niña events has not changed during the same period. As a result, they argued, the warming trend observed in the central Pacific is a result of the increasing frequency and intensity of the CP El Niño, rather than the other way around. Second, *McPhaden et al.* [2011] found the Pacific background state during the most recent decade (2000–2010) has a steeper equatorial thermocline and stronger trade winds than during earlier decades (1980–1999), which are opposite from the background states changes expected by *Yeh et al.* [2009] should anthropogenic warming be the cause for the change in the ENSO type. This inconsistency implies that the change in ENSO type may be a manifestation of natural variability. *McPhaden et al.* [2011] also interpreted the Pacific background state during 2000–2010 to be a result, rather than a cause, of the shift of the ENSO from the EP type to the CP type. Their argument is that change in the central location of the ENSO SST anomalies can project onto the changes in the background states.

1.2.3.2. ENSO–Mean State Interaction. Earlier studies have suggested that ENSO can force changes in the tropical Pacific background state [e.g., *Rodgers et al.,* 2004; *Schopf and Burgman*, 2006; *Sun and Yu,* 2009; *Choi et al.,* 2009]. Due to nonlinearities in ENSO dynamics, it is known that asymmetries exist in the intensity, frequency, or spatial structures of the warm (El Niño) and cold (La Niña) phases of the cycle. For example, strong El Niño events tend to reach a larger intensity than strong La Niña events [*Hannachi et al.,* 2003; *An and Jin,* 2004; *Duan et al.,* 2008; *Frauen and Dommenget,* 2010; *Su et al.,* 2010]. Also, strong El Niño events tend to be located more in the eastern Pacific while strong La Niña events tend to be located more in the central Pacific [*Monahan,* 2001; *Hsieh,* 2004; *Rodgers et al.,* 2004; *Schopf and Burgman*, 2006; *Sun and Yu,* 2009]. Because of these asymmetries, the positive and negative anomalies associated with the El Niño and La Niña phases may produce a nonzero residual effect on the time-mean state of the tropical Pacific. *Sun and Zhang* [2006] also conducted numerical experiments using a coupled model with and without ENSO to show that ENSO works as a basin-scale mixer on the time-mean thermal stratification in the upper equatorial Pacific. The mean state change associated with decadal ENSO variability is one of the leading modes of tropical Pacific decadal variability in many coupled atmosphere-ocean models [*Rodgers et al.,* 2004; *Yeh and Kirtman*, 2004; *Yu and Kim,* 2011b].

Sun and Yu [2009] suggested an ENSO–mean state interaction mechanism to explain how the ENSO type may shift between the EP and CP types on decadal timescales.

A key element in their hypothesized mechanism is that strong El Niño events tend to be of the EP type, whereas strong La Niña events tend to be of the CP type. In contrast, weak El Niño events tend to be of the CP type, whereas weak La Niña events tend to be of the EP type. They verified this reversed spatial asymmetry characteristic using observed ENSO events during the 1880–2006 period in two reconstructed SST datasets. During strong ENSO periods or decades, strong El Niño events are located in the eastern tropical Pacific and strong La Niña events in the central tropical Pacific. This spatial asymmetry between El Niño and La Niña can gradually reduce the background east-west SST gradient to weaken the ocean-atmosphere coupling and to shift the background state toward one favoring a weak ENSO regime. Conversely, during the weak ENSO periods or decades, weak El Niño events are located in the eastern tropical Pacific and weak La Niña events in the central tropical Pacific, which can gradually increase the east-west SST gradient, strengthen the ocean-atmosphere coupling, and shift the background state toward one favoring a strong ENSO regime. The reversed spatial asymmetries between El Niño and La Niña enable ENSO to force the tropical Pacific mean state in opposite ways between the strong and weak ENSO regimes, acting as a restoring force to push the mean state back and forth between states that sustain strong and weak ENSO intensities. ENSO can also alternate between the EP and CP types on decadal timescales. *Choi et al.* [2012] have noted such an ENSO–mean state interaction mechanism and its associations with the ENSO types and Pacific background states in coupled model simulations.

1.2.3.3. The Pacific Decadal Oscillation. Decadal changes in ENSO properties can also be associated with forcing external to the tropical Pacific, such as that related to slow SST oscillations in the North Pacific, Atlantic, or Indian oceans [e.g., *Gu and Philander*, 1997; *Behera and Yamagata,* 2003; *Verdon and Franks*, 2006; *Luo et al.,* 2005; *Dong et al.,* 2006]. One of the most well-known forcing of this kind is related to the Pacific Decadal Oscillation (PDO) [*Zhang et al.,* 1997; *Mantua et al.,* 1997], which is a leading mode of decadal SST variability in the North Pacific. Earlier studies considered the PDO a physical mode of climate variability that results from atmosphere-ocean coupling within the North Pacific [e.g., *Latif and Barnet*, 1994; *Alexander and Deser*, 1995]. More recent views consider it not a single physical mode but a combination of several processes operating on various timescales (see a review by *Newman et al.* [2015]). It has been suggested that the PDO is capable of modulating the ENSO properties by influencing the tropical Pacific background states through ocean subduction, thermocline ventilation, or atmospheric teleconnections [e.g., *McCreary and Lu*, 1994; *Gu and Philander,* 1995; *Wang and Weisberg*, 1998; *Zhang et al.,* 1998; *Barnett et al.,* 1999; *Pierce et al.,* 2000; *Chang et al.,* 2001; *McPhaden and Zhang,* 2002]. During the period of reliable instrumental records, the PDO shifted its phase twice: from a negative to a positive phase around 1976–1977 and back to a negative phase around 1999–2000. Along with the 1976–1977 phase shift, the background SSTs increased in the eastern and central tropical Pacific. This background state change was accompanied by noticeable changes in ENSO frequency and intensity [e.g., *Trenberth and Hoar*, 1996; *Rajagopolan et al.,* 1997]. Specifically, ENSO amplitude increased after the shift [*An and Wang,* 2000], and the ENSO frequency increased from being dominated by a quasi-2 yr band to a quasi-4 yr band [*Wang and Wang*, 1996]. In addition, ENSO SST anomalies were found to propagate westward before the shift but eastward after the shift [*Wang and An,* 2001], and there were more frequent El Niño events and fewer La Niña events after the shift [*Trenberth and Hoar,* 1996]. However, there was no noticeable change in the ENSO type across the 1976–1977 climate shift.

The 1999–2000 phase shift of the PDO is closer to the time that the occurrence frequency of the CP ENSO began to increase, which was suggested to be sometime around the 1980s [*Ashok et al.,* 2007], the 1990s [*Yu et al.,* 2012a], or the beginning of the 21st century [*Lee and McPhaden,* 2010; *McPhaden et al.,* 2011]. Associated with this PDO phase shift, a late-1990s climate shift has also been suggested to occur in the Pacific Rim [e.g., *Minobe*, 2000; *Peterson and Schwing*, 2003]. Dramatic changes around 1999 were reported in the North Pacific sea level pressure (SLP), SST and sea level patterns [*Minobe,* 2000; *Cummins et al.,* 2005], and in the northeastern Pacific ecosystems [*Peterson and Schwing*, 2003]. In the western North Pacific, tropical cyclone activity abruptly increased after 2000 [*Tu et al.,* 2009; *He et al.,* 2015]. Over the neighboring continents, precipitation patterns changed after the late 1990s over North and South America [*Huang et al.,* 2005] and over China [*Zhu et al.,* 2011; *Xu et al.,* 2015]. Surface temperatures in the Tibetan Plateau suddenly increased during the late 1990s [*Xu et al.,* 2009]. A La Niña-like background pattern appeared in the tropical Pacific [e.g., *McPhaden et al.,* 2011; *Chung and Li*, 2013; *Hu et al.,* 2013; *Xiang et al.,* 2013; *Kumar and Hu*, 2014], characterized by a steeper equatorial thermocline slope [*McPhaden et al.,* 2011] and strengthened Walker circulation [*Chung and Li*, 2013; *Dong and Lu*, 2013]. The breakdown of the subsurface ocean variability–ENSO relationship [*McPhaden*, 2008, 2012; *Horri et al.,* 2012] and a coherent weakening of tropical ocean-atmosphere variability [*Hu et al.,* 2013] after 2000 are likely associated with the decreases in ENSO forecast skill since 1999–2000 [*Barnston et al.,* 2012; *Xue et al.,*

2013]. Beyond the Pacific, changes in the SST and sea ice variability over the Bering and Chukchi seas [*Minobe,* 2002; *Yeo et al.,* 2014] and in the southern ocean SST variability modes [*Yeo and Kim,* 2015] have also been found after the late 1990s.

1.2.3.4. The Atlantic Multidecadal Oscillation. In addition to the PDO-related late-1990s climate shift, there is evidence that the Pacific also experienced a basin-wide climate shift in the early-1990s that can also be responsible for the change in the type of ENSO. As shown in Figure 1.1, the EP ENSO has an SST anomaly pattern that spans the tropical eastern and central Pacific. During this type of ENSO, SST variations in the central Pacific (i.e., the Niño-4 region) have an in-phase association with the SST variations in the eastern Pacific (i.e., the Niño-3 region). During the CP ENSO, the association between SST anomalies in the central Pacific and the eastern Pacific is weaker. Instead, the SST variations in the tropical central Pacific are more related to SST variations in the northeastern subtropical Pacific that are induced by an interannual atmospheric variability mode, the so-called North Pacific Oscillation (NPO) [*Walker and Bliss*, 1932; *Rogers*, 1981; *Linkin and Nigam*, 2008]. The NPO is the second leading mode of the North Pacific SLP variability and is characterized by out-of-phase SLP fluctuations between the Aleutian low and the Pacific subtropical high. Based on these features, *Yu et al.* [2012a] used three oceanic and atmospheric indices and found that the SST variations in the tropical central Pacific (i.e., the Niño-4 index) are strongly related to the SST variations in the tropical eastern Pacific (i.e., the Niño-3 index) before the early 1990s but more closely related to the SLP variations associated with NPO (i.e., the NPO index) afterward. They concluded that the change in ENSO from the EP type to the CP type occurred in the early 1990s. This climate shift resulted in a change in ENSO location from the eastern Pacific to the central Pacific. *Yu et al.* [2015a] further revealed that the early-1990s climate shift was related to the Atlantic Multidecadal Oscillation (AMO) [*Schlesinger and Ramankutty,* 1994; *Kerr*, 2000], which changed from a negative phase to a positive phase in the early 1990s as well. The AMO is characterized by slow changes in SST in the North Atlantic and is believed to have a period of 60–80 yr. Although there is still ongoing debate on the causes of the AMO, it is agreed that the slow variability mode influences climate not only within the Atlantic basin but also across the entire Northern Hemisphere, including the Pacific basin [e.g., *Dong et al.,* 2006; *Zhang and Delworth*, 2007]. The physical processes that link the NPO and AMO to the CP ENSO are described in detail in section 1.3.

Evidence of the early-1990s climate shift in the Pacific has also been found in other climate phenomena of the low-latitude Pacific. In the western Pacific, upper ocean currents and sea level structure also changed around this time, with the north equatorial current and the north equatorial countercurrent migrating southward [*Qiu and Chen*, 2012] and sea level rise accelerating to a rate not seen in the preceding several decades [*Merrifield*, 2011]. These oceanic state changes were accompanied by changes in trade wind patterns [*Qiu and Chen*, 2012]. *Sui et al.* [2007] found that the interannual variability of the western Pacific subtropical high was dominated by frequencies of 3–5 yr before the early 1990s but 2–3 yr afterward. The relationships between the Asian monsoon and the other monsoon systems in the Northern Hemisphere (e.g., the North American and North African monsoons) changed in such a way that the interannual rainfall variability produced by these the monsoon systems decreased dramatically after 1993 [*Lee et al.,* 2014]. The relationships between the East Asian winter monsoon and ENSO also undergo low-frequency oscillation [*Zhou et al.,* 2007]. Moreover, the typical drought pattern in China was replaced by a new pattern after the early 1990s [*Qian et al.,* 2014]. These recent studies together indicate that the Pacific climate shift in the early 1990s affected the ENSO location, the monsoons, the subtropical high, and the subtropical ocean gyre.

1.2.3.5. Random Forcing. Other mechanisms have also been put forth to explain the increased occurrence of the CP ENSO during the past few decades. *Newman et al.* [2011] used a linear inverse modeling technique to suggest that natural random variations in the atmosphere can project onto two particular initial SST anomaly patterns, each of which can eventually develop into either the EP or CP type of ENSO through thermocline and zonal advection feedbacks, respectively. They argued that such natural random variations can result in a slow alternation in the type of ENSO without the need for changes in the background state.

1.3. CHANGES IN ENSO DYNAMICS

1.3.1. The Different Generation Mechanisms for the Two Types of ENSO

The fundamental dynamics of ENSO have been traditionally believed to reside mostly within the tropical Pacific [*Neelin et al.,* 1998; *Philander* 1999; *Wang et al.,* 2015; and the references therein]. The prevailing ENSO theories emphasize the delayed response of subsurface ocean to atmospheric forcing for the oscillation of ENSO. In this view, the delayed oceanic response results from the propagation and reflection of oceanic waves along the equator in the delayed oscillator theory [*Suarez and Schopf* 1988; *Battisti and Hirst* 1989], the adjustment of

the nonequilibrium between zonal-mean thermocline depth and wind forcing in the recharged oscillator theory [e.g., *Wyrtki* 1975; *Zebiak* 1989; *Jin* 1997], or the lagged response of western Pacific wind stress to ENSO SST anomalies in the western Pacific oscillator theory [*Weisberg and Wang* 1997; *Wang et al.,* 1999]. Variations in ENSO properties (such as its low-frequency and quasibiennial periodicity) can be produced by these delayed atmosphere-ocean coupling processes and their interactions with the annual cycle or by the nonlinear chaotic characteristics of these ENSO dynamics [*Jin et al.,* 1994; *Jin* 1996, 1997; *Tziperman et al.,* 1994, 1995; *Chang et al.,* 1995, 1996; *Mantua and Battisti* 1995; *An and Jin*, 2001]. From this point of view, the various types of ENSO do not necessarily represent distinct ENSO dynamics. However, recent studies of the EP and CP types of ENSO have begun to suggest that these two types of ENSO are likely to have different underlying dynamics [e.g., *Kao and Yu,* 2009; *Yu et al.,* 2011; *Yu and Kim*, 2011a; *S.-T. Kim et al.,* 2012; *Yu et al.,* 2012a; *Lin et al.,* 2014]. In this framework, the EP ENSO is produced by the traditional ENSO dynamics, while the generation of the CP ENSO relies more on forcing from the subtropical Pacific and its interaction with ocean mixed-layer dynamics in the equatorial central Pacific.

As shown in Figure 1.2, the composite CP ENSO is associated with in situ subsurface ocean temperature anomalies that do not show the basinwide propagation characteristics typical of the delayed oscillator theory [*Suarez and Schopf* 1988; *Battisti and Hirst* 1989]. *Yu and Kim* [2010b] further examined the thermocline variations associated with nine major CP El Niño events since 1960. Three of the CP El Niño events (i.e., 1968–1969, 1990–1991, and 1991–1992) they examined undergo a prolonged decaying phase (Fig. 1.3a) that decays slowly and is followed by a warm event in the eastern Pacific. Figure 1.3d shows that the mean thermocline depth (represented by the 20 °C isotherm) for this group of events (i.e., Group 1) is deeper than normal in the equatorial Pacific (i.e., recharged state), which later gives rise to an EP El Niño to prolong the decay of these three CP El Niño events. The other three CP El Niño events (1963–1964, 1977–1978, and 1987–1988) occurred in the presence of shallow-than-normal thermoclines (i.e., discharged state; Group 2 of Fig. 1.3d). This group of CP El Niño events is followed by a La Niña event in the eastern Pacific, resulting in an abrupt termination of the CP El Niño (Fig. 1.3b). The last three events (1994–1995, 2002–2003, and 2004–2005) occurred with near-normal thermocline depths (i.e., neutral state; Group 3 of Fig. 1.3d). This group of events undergoes a symmetric-decaying pattern, whose SST anomalies grow and decay symmetrically with respect to a peak phase (Fig. 1.3c). Therefore, CP El Niño events can occur when the equatorial Pacific thermocline is above, below, or near the normal depth, as also suggested by a recent modeling study [*Fedorov et al.,* 2014]. This finding further confirms that the generation of CP ENSO does not depend on thermocline dynamics. However, these different thermocline structures do affect whether a warming, cooling, or neutral event may occur in the eastern Pacific as the CP event decays. Depending on the thermocline structure, the eastern Pacific warming, or cooling may interact with the SST evolution of the CP event and give rise to the three distinct evolution patterns of CP El Niño. Although the thermocline variations are not crucial to the generation and the dynamics of the CP type of El Niño, the state of the thermocline at the peak phase of a CP ENSO event can potentially be used to predict when and how the CP ENSO event will terminate. It is the interplay between the dynamics of the CP and EP types of ENSO that makes the thermocline information useful for the prediction of both types of SST variations.

1.3.2. The Central-Pacific ENSO: Extratropical Atmospheric Forcing Mechanism

As mentioned, for the CP El Niño the equatorial westerly anomalies appear to the west of the positive SST anomalies in the central Pacific and the equatorial easterly anomalies to the east. *Ashok et al.* [2007] argued that the thermocline variations induced by this wind anomaly pattern are responsible for the generation of the CP ENSO. The equatorial westerly anomalies induce downwelling Kelvin waves propagating eastward and the equatorial easterly anomalies induce downwelling Rossby waves propagating westward and, together, they deepen the thermocline in the central Pacific to produce the CP El Niño. *Kug et al.* [2009] emphasized the fact that the equatorial easterly anomalies can suppress warming in the eastern Pacific during a CP El Niño event by enhancing upwelling and surface evaporation. However, they also argued that the mean depth of thermocline in the central Pacific is relatively deep and the wind-induced thermocline variations may not be efficient in producing the CP SST anomalies. Instead, they suggested that ocean advection is responsible for the development of the central Pacific warming. *Yu et al.* [2010] also concluded that the SST anomalies of the CP ENSO undergo rapid intensification through ocean advection processes. However, they showed that the initial establishment of the CP SST anomalies is related to forcing from the extratropical atmosphere and subsequent atmosphere-ocean coupling in the subtropics.

Yu et al. [2010] performed an analysis of the near-surface ocean temperature budget to identify the physical processes involved in the development of the CP ENSO. They showed that the SST anomalies associated

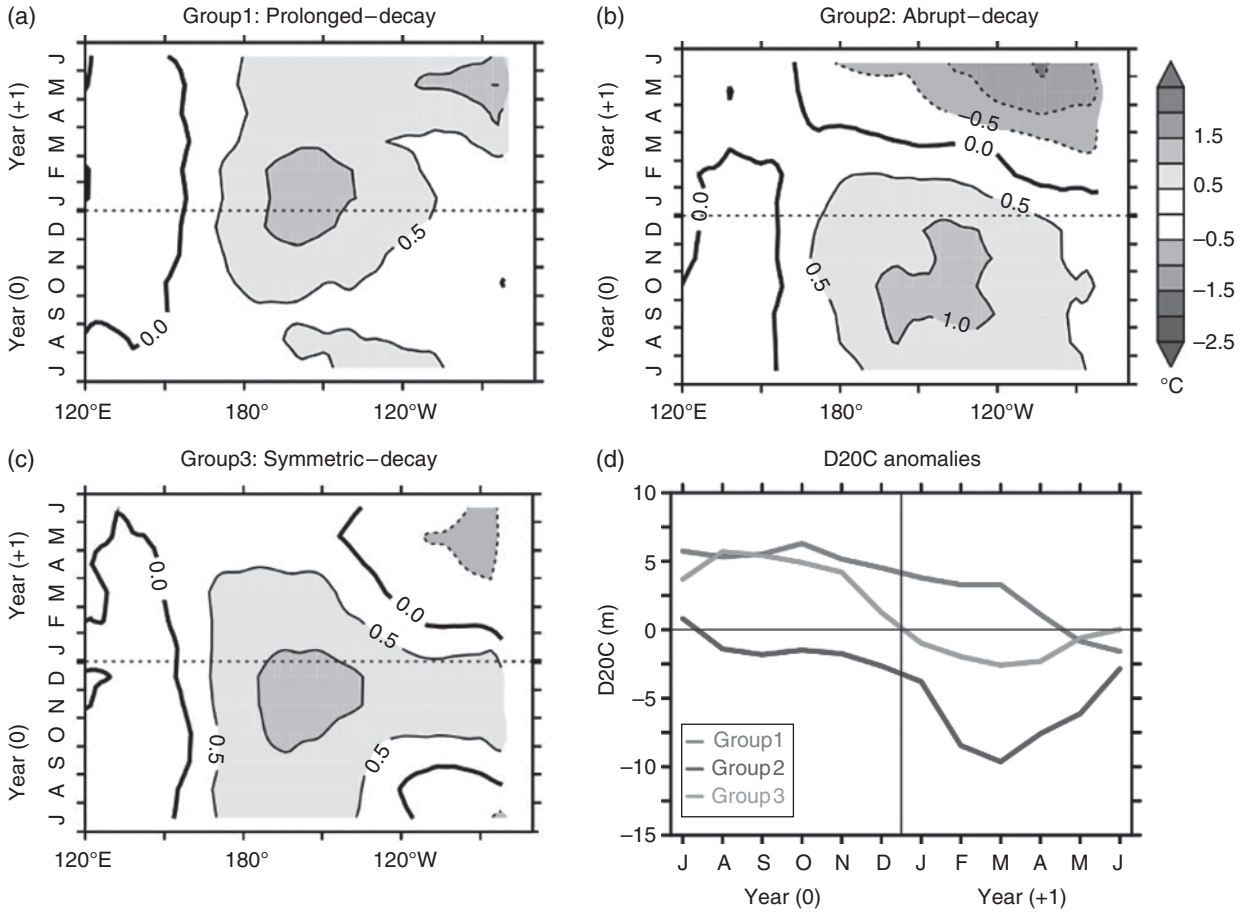

Figure 1.3 Evolution of composite equatorial Pacific (5°S–5°N) SST anomalies for (a) the group of CP El Niño events that has a prolonged decay (i.e., 1968–1969, 1990–1991, and 1991–1992), (b) the group that has an abrupt decay (i.e., 1963–1964, 1977–1978, and 1987–1988), and (c) the group that has a symmetric decay (i.e., 1994–1995, 2002–2003, and 2004–2005). The evolution is shown from July of the El Niño year (0) to June of the following year (+1) and is calculated from the Extended Reconstruction of Historical Sea Surface Temperature dataset (ERSST) [*Smith et al.,* 2008]. Panel (d) shows the evolution of the depth anomalies of the zonal-mean 20 °C isotherm (D20C) at the equator (5°S–5°N) for the three groups of events. The zonal mean is averaged between 120°E and 80°W and is calculated using the Simple Ocean Data Assimilation Reanalysis data (SODA) [*Carton et al.,* 2000]. Adapted from *Yu and Kim* [2010b].

with the CP ENSO undergo rapid intensification in the equatorial central Pacific through local atmosphere-ocean interactions, which involve only mixed layer ocean dynamics and are similar to those described for the slow-SST mode of ENSO [*Neelin* 1991; *Neelin and Jin* 1993]. This mode requires surface wind anomalies to induce anomalous air-sea fluxes and ocean advection processes to intensify the initial SST perturbation. *Yu et al.* [2010] suggested that the initial SST anomalies in the central equatorial Pacific were, however, established by forcing from the extratropical atmosphere. This suggestion is supported by regressions of the Pacific SST anomalies onto the CP ENSO index. As shown in Figure 1.4, the regressed positive SST anomalies appear first in the northeastern subtropical Pacific and later spread toward the central equatorial Pacific to initiate ENSO event in the central Pacific.

The possibility of subtropical precursors in triggering ENSO events has long been recognized. However, recent studies on CP ENSO dynamics have begun to emphasize that these subtropical processes are not just precursors of ENSO but an essential element in the generation of CP ENSO events. As revealed by Figure 1.4, the CP ENSO is preceded by SST anomalies in the northeastern Pacific, which are characterized by a band of SST anomalies extending typically from Baja California toward the equatorial central Pacific. As the subtropical SST anomalies approach the equatorial Pacific, El Niño events develop and begin to grow. Several recent studies [e.g., *Vimont et al.,* 2003; *Anderson*, 2004; *Yu and Kim*, 2011a]

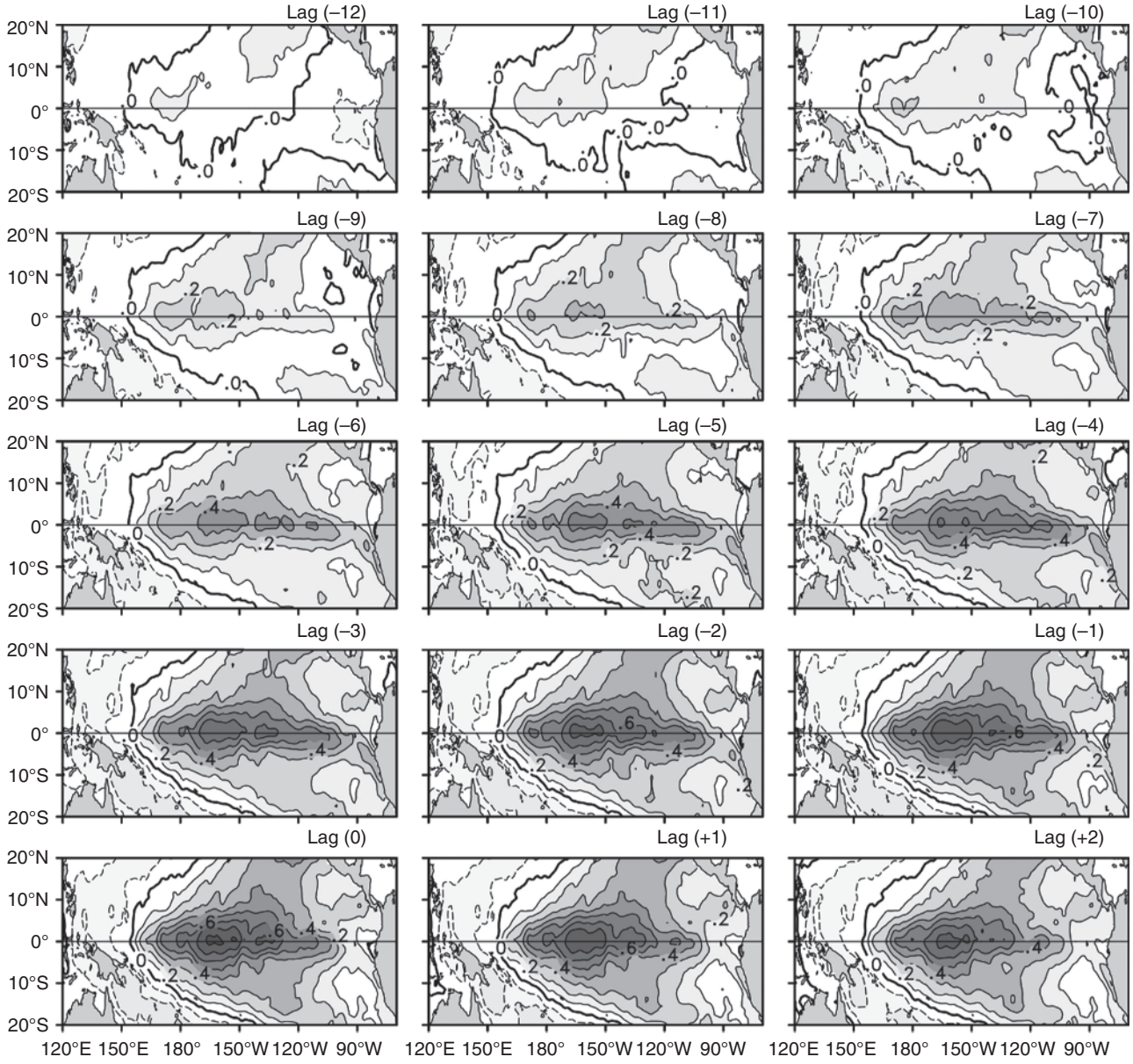

Figure 1.4 Evolution of tropical Pacific SST anomalies of the CP ENSO. Values shown are SST anomalies regressed on the CP ENSO index from a lag of −12 mo to a lag of +2 mo. The contour interval is 0.1 °C. The HadISST dataset for the period 1948–2010 is used.

have suggested that the initial warming off Baja California is forced by atmospheric fluctuations, particularly those associated with NPO. When the Pacific SST anomalies are regressed onto the NPO index (Fig. 1.5), it is obvious that the NPO first induces positive SST anomalies off Baja California via surface heat fluxes. The SST anomalies then extend southwestward toward the tropical Pacific. After the SST anomalies reach the tropical Pacific, an El Niño event occurs and develops there. The evolution shown in Figure 1.5 is very similar to the evolution of SST anomalies shown in Figure 1.4 preceding the development of a CP El Niño event. This similarity offers evidence that there exists a close relationship between the subtropical Pacific precursors and CP ENSO.

Ocean-atmosphere coupling in the subtropical Pacific is crucial for the spread of the NPO-induced SST anomalies southward into the deep tropics. The coupling processes begin as the SST anomalies off Baja California feed back onto and modify near surface winds via convection. The wind anomalies induced by the convection tend to be located to the southwest of initial subtropical SST anomalies [*Xie and Philander,* 1994], where new positive

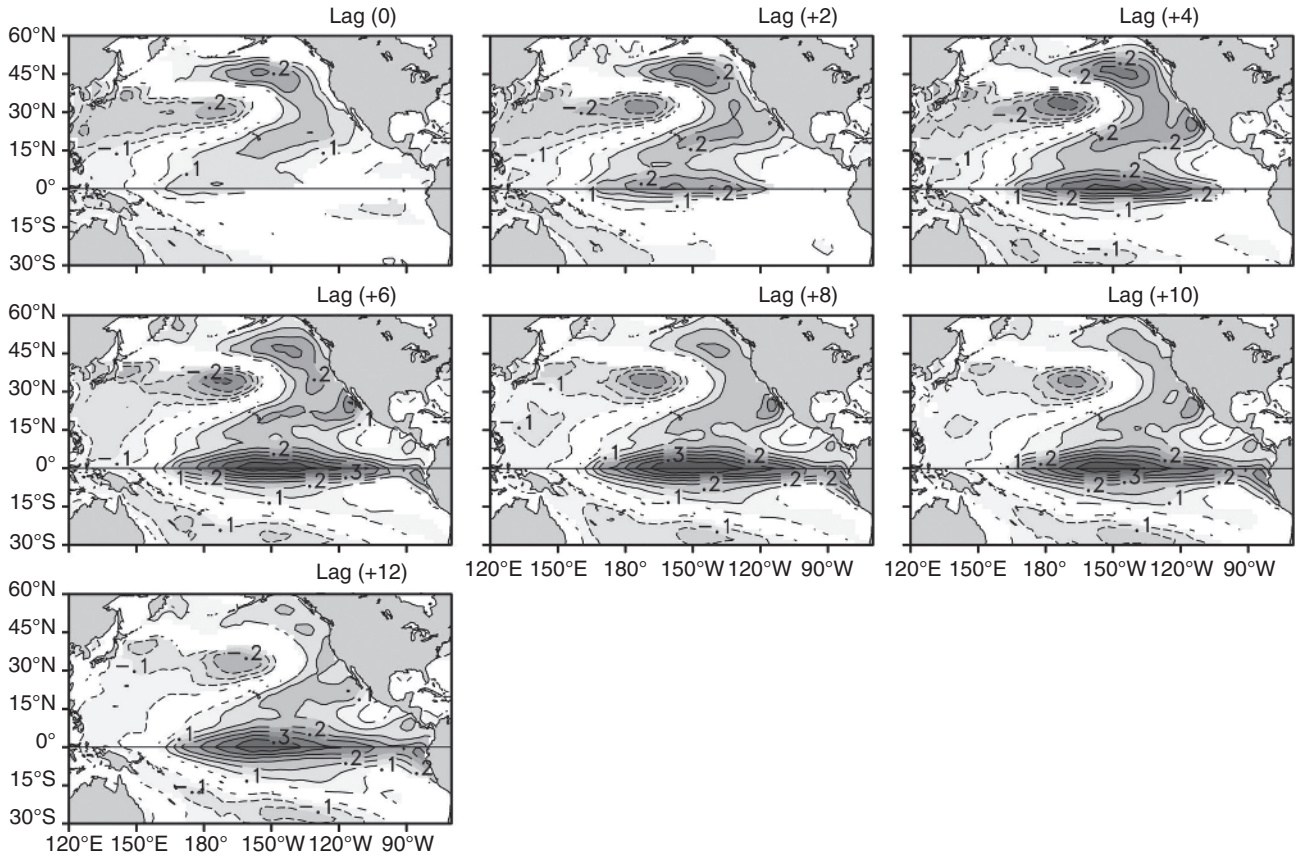

Figure 1.5 SST anomalies regressed on the NPO index from a lag of 0 mo to a lag of +12 mo. The contour interval is 0.05 °C and only the coefficients exceeding the 99% confidence level are shown. Positive lags denote that the NPO leads the SST anomalies. The National Centers for Environmental Prediction/National Center for Atmospheric Research (NCEP/NCAR) reanalysis [*Kalnay et al.,* 1996] and HadISST datasets for the period of 1948–2010 are used.

SST anomalies can be formed through a reduction in evaporation. The atmosphere then continues to respond to the new SST anomalies by producing wind anomalies farther southwestward. Through this wind-evaporation-SST (WES) feedback [*Xie and Philander,* 1994], the SST anomalies initially induced by the NPO off Baja California can extend southwestward into the deep tropics. This series of subtropical Pacific coupling processes is referred to as the seasonal footprinting mechanism [*Vimont et al.,* 2001, 2003, and 2009]. This mechanism also offers a way to explain how the subtropical SST anomalies can be sustained from boreal winter, when extratropical atmospheric variability (e.g., the NPO) is largest, to the following spring or summer to excite CP ENSO events.

As mentioned, the SST anomaly pattern of the subtropical precursor to ENSO (in particular, the CP ENSO) strongly resembles the PMM that is the leading coupled variability mode of the subtropical Pacific. A strong association between the spring PMM index and the following winter's ENSO index was demonstrated in *Chang et al.* [2007], who found that a majority of El Niño events over the past four decades were preceded by SST and surface wind anomalies similar to those associated with the PMM. Recently, the winter SST anomalies in the western North Pacific have been suggested as a subtropical ENSO precursor, which precede ENSO development in the following year [*S.-Y. Wang et al.,* 2012, 2013]. There are several ways to link these ENSO precursor-associated anomalies to the generation of ENSO events in the equatorial Pacific. One explanation emphasizes how the surface wind anomalies associated with the subtropical precursor can directly or indirectly (through the reflection of off-equatorial Rossby wave in the western Pacific) excite downwelling Kelvin waves along the equatorial thermocline that propagate eastward to trigger El Niño events in the eastern Pacific [e.g., *Alexander et al.,* 2010; *S.-Y. Wang et al.,* 2012, 2013]. This view appears more related to the onset of EP ENSO events. However, when the subtropical precursor reaches the equatorial Pacific, it can also force a CP ENSO event by interacting with the local ocean mixed layer. Figure 1.6 illustrates this view of how the underlying dynamics of the two types of ENSO

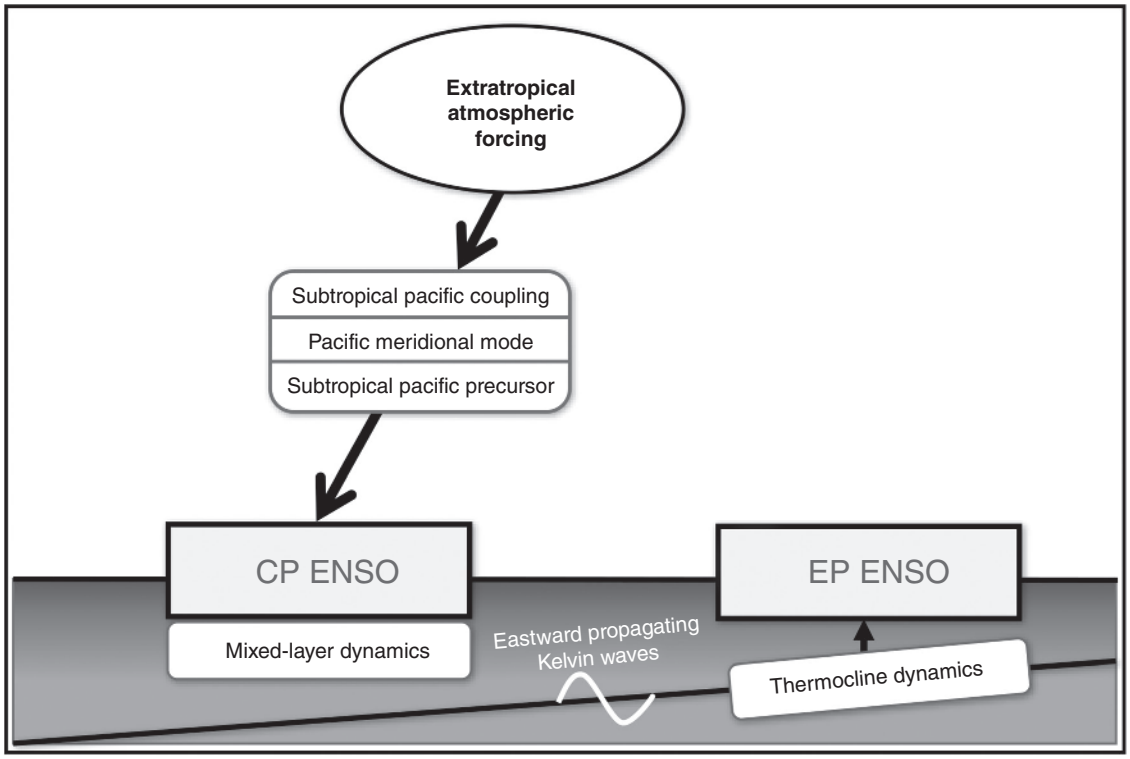

Figure 1.6 A schematic diagram illustrating the possible relationships between the subtropical Pacific precursors and the two types of ENSO (CP and EP). (*See insert for color representation of the figure.*)

can interact with the subtropical Pacific precursor. In this view, the generation of the CP ENSO is more related to mixed layer ocean dynamics. *Dommenget* [2010] and *Clement et al.* [2011] have demonstrated that ENSO-like events can be produced in coupled models where the ocean component consists of a mixed layer only without any thermocline dynamics. The generation of the EP ENSO is considered more related to the thermocline dynamics depicted by the delayed-oscillator [*Suarez and Schopf* 1988; *Battisti and Hirst* 1989] and charge-recharged oscillator theories [e.g., *Wyrtki* 1975; *Zebiak* 1989; *Jin* 1997].

1.3.3. Links Between the Atlantic Multidecadal Oscillation and the Central-Pacific ENSO

The strength of the subtropical Pacific coupling, therefore, plays a key role in determining how efficiently the subtropical Pacific precursors can penetrate into the tropics to excite ENSO events, particularly CP ENSO events. As mentioned, *Yu et al.* [2012a] found that the early 1990s is the time when ENSO changed from the EP type to the CP type. *Yu et al.* [2015a] further confirmed that the subtropical Pacific coupling was stronger after the early 1990s. They analyzed the subtropical Pacific coupling strength by examining the correlation coefficient between the SST and surface wind anomalies associated with the PMM. As shown in Figure 1.7, the coupling strength was at a relatively constant level before and after the 1976–1977 climate shift, which suggests that the phase change in the PDO cannot affect the subtropical Pacific coupling. In contrast, the subtropical Pacific coupling strength increased after the early-1990s climate shift. The stronger subtropical Pacific coupling has made it easier for the subtropical precursors to penetrate into and to influence the deep tropics, and, as a result, the occurrence of CP ENSO events increases. As mentioned, the early-1990s climate shift is related to the phase change of the AMO. *Yu et al.* [2015a] coupled an atmospheric general circulation model (AGCM) with a slab ocean model to demonstrate the relationship between the AMO and the CP ENSO. In the coupled model, they prescribed a positive phase of the AMO SST anomalies in one experiment and a negative phase of the AMO in the other experiment. They showed that the Pacific SST variability produced by the coupled model increased most in the tropical central Pacific when a positive AMO was prescribed in the Atlantic. They also laid out the chain of events to explain how the AMO influenced the CP ENSO. First, a switch of the AMO to its positive phase in the early 1990s led to an intensification of the Pacific subtropical high. The intensified high resulted in stronger-than-average

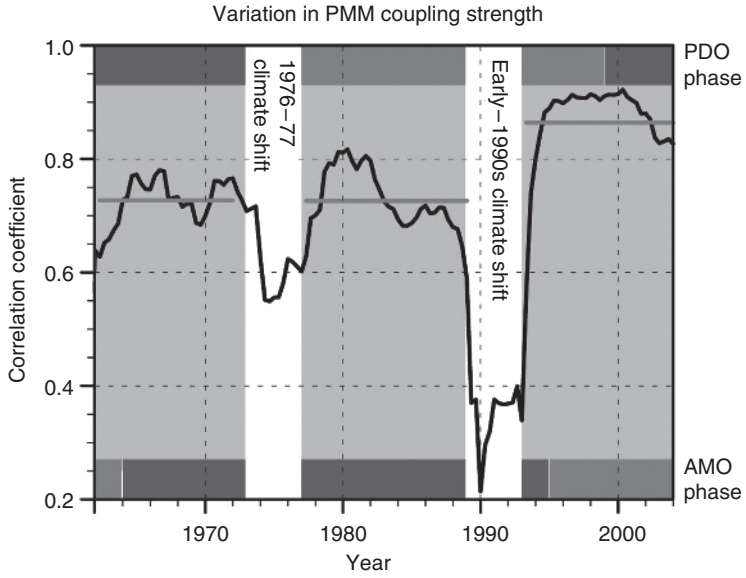

Figure 1.7 Coefficients of the 10 yr running correlation between the PMM-SST and PMM-wind indices in boreal spring (March–May). The ERSST and NCAR/NCEP reanalysis datasets are used. The red line indicates the mean of the correlation coefficients during each period. The shading at the top and bottom show the phases (positive red/negative blue) of the PDO and the AMO, respectively. Modified from *Yu et al.* [2015a].

background trade winds that enhanced the WES feedback mechanism, strengthening the subtropical Pacific coupling between the atmosphere and ocean, making the subtropical Pacific precursors more capable of penetrating into the deep tropics, and ultimately leading to increased occurrence of CP ENSO events. The study of *Yu et al.* [2015a] suggests that the recent shift from more conventional EP to more CP type of ENSO events can thus be at least partly understood as a Pacific Ocean response to the phase change in the AMO.

1.3.4. The Roles of the Hadley and Walker Circulations

The emergence of CP ENSO represents a change in ENSO dynamic from one that emphasizes the tropical Pacific coupling processes to another that emphasizes the subtropical Pacific forcing. This recent change in ENSO dynamic can also be understood via the different roles played by the Walker and Hadley circulations in the ENSO dynamic, as noted by *Yu et al.* [2010]. Figure 1.8 shows the correlation coefficients between SLP anomalies and the EP and CP ENSO indices. The EP ENSO is associated with a southern-oscillation pattern characterized by out-of-phase SLP anomalies between the eastern and western tropical Pacific. The SLP variations over the maritime continent region are linked to SLP over the eastern equatorial Pacific through the Walker circulation. The SLP anomaly pattern associated with CP ENSO does not really resemble the Southern Oscillation. Instead, the SLP variations over the maritime continent are linked to SLP variations in the subtropics of both the North and South Pacific, suggesting that a connection through local Hadley circulation may be more important. Therefore, *Yu et al.* [2010] argued that the tropical Pacific Ocean interacts with the Walker circulation to produce EP ENSO but the local Hadley circulation to produce CP ENSO. The alternation between the EP and CP types of ENSO can be viewed as a result of changes in the relative strengths of the Hadley and Walker circulations. A stronger Walker circulation may lead to a dominance of the EP type, while a stronger Hadley circulation may favor the CP type. This view was further examined in *Yu et al.* [2012a], in which they compared the strength of the time-mean Walker and Hadley circulations before and after the early-1990s climate shift. Consistent with the view of *Yu et al.* [2010], the period of postclimate shift has a stronger mean Hadley circulation compared to the period of preclimate shift. The stronger Hadley circulation could help the NPO-induced SST variations to spread into the tropical central Pacific. In association with the changes in the strength of mean atmospheric circulations, the tropical central Pacific has become more responsive to the forcing and influence from the extratropical atmosphere, which has resulted in more frequent occurrence of CP ENSO events. The relative dominance of the two types of ENSO may be related to the relative strength of the Hadley and Walker circulations. As for the mean strength of the Walker circulation, it is in debate whether it has weakened [e.g., *Vecchi et al.,* 2006; *Vecchi and Soden,* 2007; *Xie et al.,* 2010; *Tokinaga et al.,* 2012; *Yu et al.,* 2012a] or strengthened

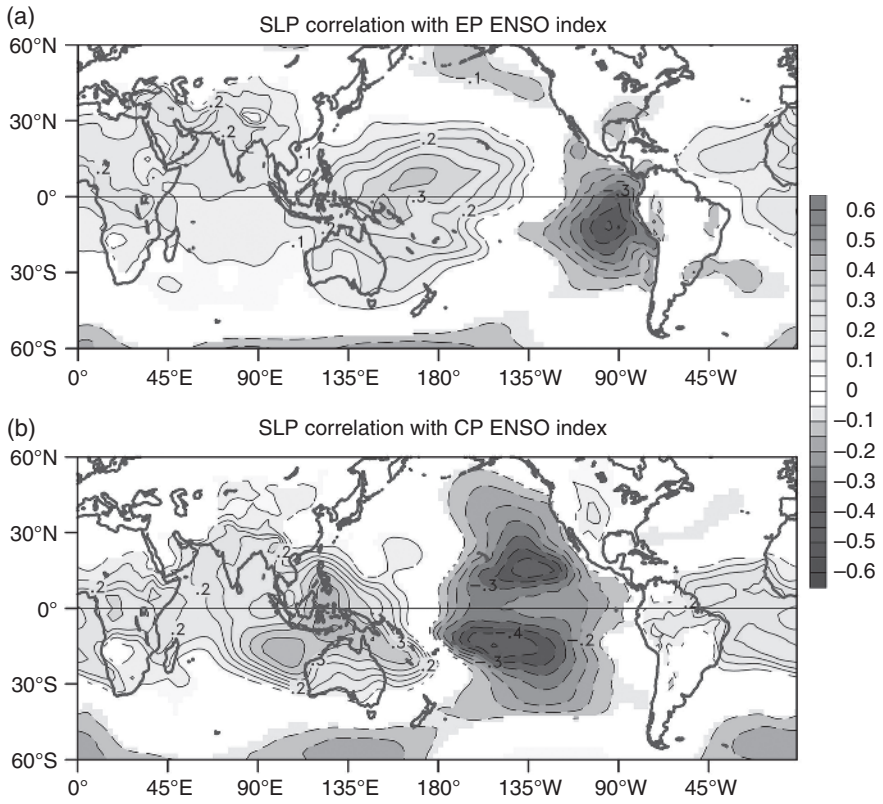

Figure 1.8 Correlation of SLP anomalies with (a) the EP and (b) CP ENSO indices. Only the coefficients exceeding the 95% confidence level are shown. The NCEP/NCAR reanalysis dataset for the period of 1948–2010 is used.

[e.g., *Dong and Lu,* 2013; *Hu et al.,* 2013; *L'Heureux et al.,* 2013] in recent decades, although it is more generally agreed that the circulation has strengthened in the most recent decade [e.g., *England et al.,* 2014].

1.3.5. Other Possible Mechanisms

In addition to the extratropical atmospheric forcing mechanism, other mechanisms have been proposed to explain the generation of the two types of ENSO. For example, *Yu et al.* [2009] used ocean-atmosphere coupled GCM (CGCM) experiments to suggest that the CP ENSO can be excited by forcing associated with the Asian and Australian monsoons. *Chung and Li* [2013] argued that the La Niña-like (stronger zonal SST gradient) decadal background state since 1999 is responsible for the more frequent occurrence of CP El Niño. Their numerical experiments showed that with the increased background zonal SST gradient, the anomalous wind and precipitation response to EP or CP SST forcing shifts to the west, leading to a westward shift in the SST anomaly tendency that resembles the CP ENSO. *Ren and Jin* [2013] found that with the decadal signal removed, the ocean heat content shows recharge-discharge processes throughout the life cycles of both ENSO types. They showed that the different zonal locations of the SST and easterly wind anomalies and the associated thermocline feedback contribute to the growth and phase transitions of the two ENSO types. This view of varying thermocline feedbacks for the two ENSO types is consistent with the study of *Hu et al.* [2012b] who suggested that the subsurface ocean temperature anomalies are weaker in the CP ENSO than in the EP ENSO. *Hu et al.* [2012b] also found differences in the westerly wind bursts (WWBs) between the two types of ENSO. They suggested that the CP (EP) ENSO is followed by weaker and more westward confined (stronger and eastward extended) WWBs along the equatorial Pacific, which are associated with suppressed (enhanced) air-sea interactions over the cold tongue/Intertropical Convergence Zone and weaker (stronger) thermocline feedbacks. *Fedorov et al.* [2014] and *Hu et al.* [2014] also reached a similar conclusion on the differences in the importance of WWB for the two ENSO types. These two modeling studies showed that the EP El Niño develops when WWBs are imposed in an initial recharge ocean state, while the CP El Niño develops in a neutral ocean state in the presence of a WWB or in a recharge state without a WWB. All these WWB studies suggest that properly accounting for the preceding westerly wind signal and air-sea interaction may be necessary for

accurate ENSO predictions [*Hu et al.,* 2012b; *Fedorov et al.,* 2014; *Hu et al.,* 2014; *D. Chen et al.,* 2015].

1.4. CHANGES IN ENSO TELECONNECTIONS AND ASSOCIATED CLIMATE EXTREMES

The recent identification of the two distinct types of ENSO offers a new way to consider the impact of ENSO on global climate. There are indications that the atmospheric response to ENSO events can be sensitive to the exact location of their SST anomalies [e.g., *Mo and Higgins* 1998; *Hoerling and Kumar*, 2002; *Barsugli and Sardeshmukh*, 2002; *DeWeaver and Nigam*, 2004; *Larkin and Harrison*, 2005b]. An increasing number of recent studies have looked into the different impacts produced by these two types of ENSO on various parts of global climate. Many of these studies have revealed that the CP ENSO can affect global climate differently from the EP ENSO [e.g., *Larkin and Harrison*, 2005b], indicating that one should not simply use the existing understanding of the conventional EP ENSO to anticipate the climate impacts and teleconnections associated with the CP ENSO. A systematic investigation of the global and regional impacts of the CP ENSO is required. In this section, we use the differing impacts of the two types of ENSO on global climate to illustrate how ENSO's teleconnection and associated climate extremes have been changing in the past few decades.

1.4.1. North America

It is well recognized that North American climate is significantly impacted by ENSO [e.g., *Ropelewski and Halpert*, 1986, 1989; *Kiladis and Diaz*, 1989; *Livezey et al.,* 1997; *Cayan et al.,* 1999; *Larkin and Harrison*, 2005b; and many others]. However, the existence of two types of ENSO was not taken into account in most of the past studies. The El Niño impact on US winter temperatures is traditionally characterized as a north-south dipole pattern, in which above normal temperatures are found over the northern states and below normal temperatures over the southern states [e.g., *Ropelewski and Halpert*, 1986]. *Larkin and Harrison* [2005a] first pointed out that seasonal US weather anomalies associated with the two types of El Niño are quite different. *Mo* [2010] considered a priori the two types of ENSO to examine ENSO's impacts on North American climate. The author contrasted the impacts of ENSO on air temperature and precipitation over the United States during the period 1915–1960 when the EP type dominated and the period 1962–2006 when the CP type had increased in importance, and concluded that the EP El Niño produced a north-south contrast pattern in the air temperature variations, similar to the traditional view. For the CP El Niño, the author found the temperature variations are characterized by more of an east-west contrast pattern with warming over the Pacific Northwest and cooling in the Southeast. *Yu et al.* [2012b] also found that the two types of ENSO produced different impacts on US winter temperature. Their result is similar to that of *Mo* [2010] but with significant differences in the details. *Yu et al.* [2012b] first separately regressed winter (January–March) surface air temperature anomalies to the EP and CP ENSO indices to show that, during EP El Niño events (Fig. 1.9a), positive winter temperature anomalies are concentrated mostly over the northeastern part of the United States and negative anomalies are most obvious over the southwestern states. During CP El Niño events (Fig. 1.9b), the warm anomalies are located in the northwestern United States and the cold anomalies are centered in the southeastern United States. The US temperature anomaly patterns are rotated by about 90° between these two types of El Niño. Adding these two impact patterns together can result in a pattern that resembles the traditional El Niño impact on the US winter temperature (i.e., a warm-north and cold-south pattern). It indicates that the traditional view of El Niño impact is likely a mixture of the impacts of the two types of El Niño. *Yu et al.* [2012b] was able to reproduce these two different impact patterns in forced model experiments performed with the Community Atmosphere Model version 4 (CAM4) [*Neale et al.,* 2013] from the National Center for Atmospheric Research (NCAR) (shown in Fig. 1.9c and d], in which SST anomalies characteristic of the EP El Niño and CP El Niño were separately used to force the model in two different sets of ensemble experiments. The regressed impact patterns can also be identified in the four strongest EP El Niño events (in 1997, 1982, 1972, and 1986) and four of the top five strongest CP El Niño events (in 2009, 1957, 2002, and 2004). Both *Mo* [2010] and *Yu et al.* [2012b] argued that the cause of the different impacts on US winter temperature is the different wave train patterns excited by these two types of El Niño in the extratropical atmosphere. The winter atmosphere produces a Pacific–North American (PNA) teleconnection pattern [*Wallace and Gutzler*, 1981] during the CP El Niño, which consists of a positive anomaly center extending from eastern Alaska to the northwestern United States and a negative anomaly center over the southeastern United States, resulting in a warm-northwest and cold-southeast pattern of temperature anomalies. During the EP El Niño, the winter atmosphere produces a poleward wave train emanating from the tropical eastern Pacific, across the southwestern United States, and into the northeastern United States, leading to the cold-southwest and warm-northeast pattern in US winter temperatures. This wave train pattern resembles the Tropical North Hemisphere (TNH) pattern [*Mo and Livezey*, 1986].

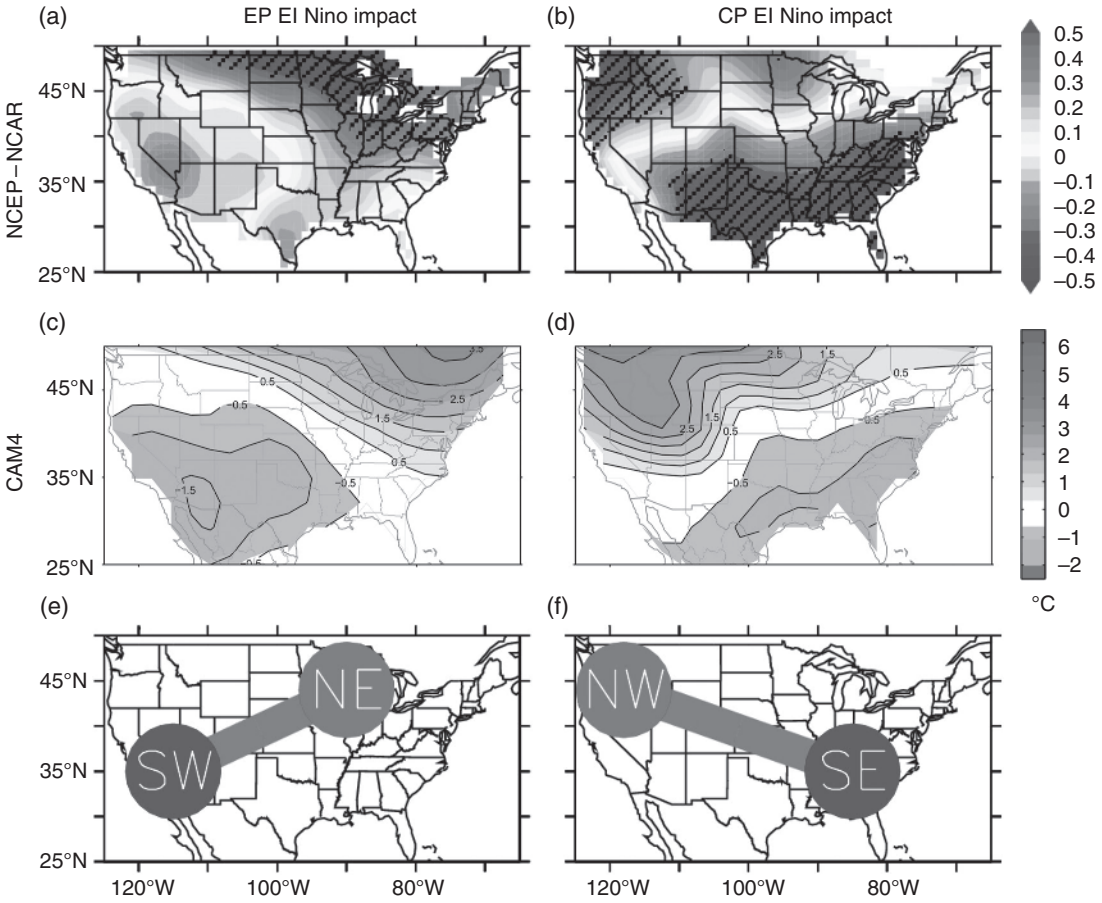

Figure 1.9 EP (left panels) and CP (right panels) El Niño impacts on US winter (January–March) surface air temperatures. Observed temperature anomalies regressed onto the (a) EP and (b) CP ENSO indices. Coefficients exceeding the 90% confidence level are dotted. The NCEP/NCAR reanalysis dataset for the period 1950–2010 is used. Temperature patterns reproduced by the Community Atmosphere Model version 4 (CAM4) in the (c) EP and (d) CP experiments. Only differences exceeding the 90% confidence level are shaded. Schematic diagrams of the (e) EP and (f) CP El Niño impacts on temperatures. Adapted from *Yu et al.* [2012b]. (*See insert for color representation of the figure.*)

Concerning the US winter precipitation, the classical view of El Niño's impact is one of negative precipitation anomalies in the northern United States and positive precipitation anomalies in the southern United States due to a southward displacement of the tropospheric jet stream and associated winter storm activity [e.g., *Ropelewski and Halpert*, 1986, 1989; *Kiladis and Diaz*, 1989; *Dettinger et al.,* 1998; *Mo and Higgins*, 1998; *Cayan et al.,* 1999]. *Mo* [2010] suggested that, during the EP El Niño events, precipitation decreases in the Pacific Northwest but increases in northern California. For the CP El Niño, its influence on precipitation increases in the Southwest but decreases in the Ohio valley compared to the EP El Niño. *Yu and Zou* [2013] regressed US winter precipitation anomalies on the EP and CP ENSO indices to identify the impact patterns (Fig. 1.10a and b). Both types of El Niño produce dry-north and wet-south anomaly patterns, similar to the seesaw pattern that has traditionally been used to describe El Niño impacts on US winter precipitation. However, the dry anomalies produced by the CP El Niño are of larger magnitude and cover larger areas than those produced by the EP El Niño. For example, the dry anomalies cover only the Great Lakes region during the EP El Niño, but extend southwestward through the Ohio-Mississippi valley toward the Gulf Coast during the CP El Niño. In contrast, the wet anomalies tend to have smaller magnitudes during the CP El Niño than during the EP El Niño, a phenomenon that is most obvious over the southeast United States. In Figure 1.10, a and b indicate that the CP El Niño tends to intensify the dry anomalies but weaken the wet anomalies of the impact pattern produced by the EP El Niño. This important difference is clearly revealed in Figure 1.10c, where the precipitation anomalies regressed on the EP El Niño were subtracted from the anomalies regressed in the CP El Niño.

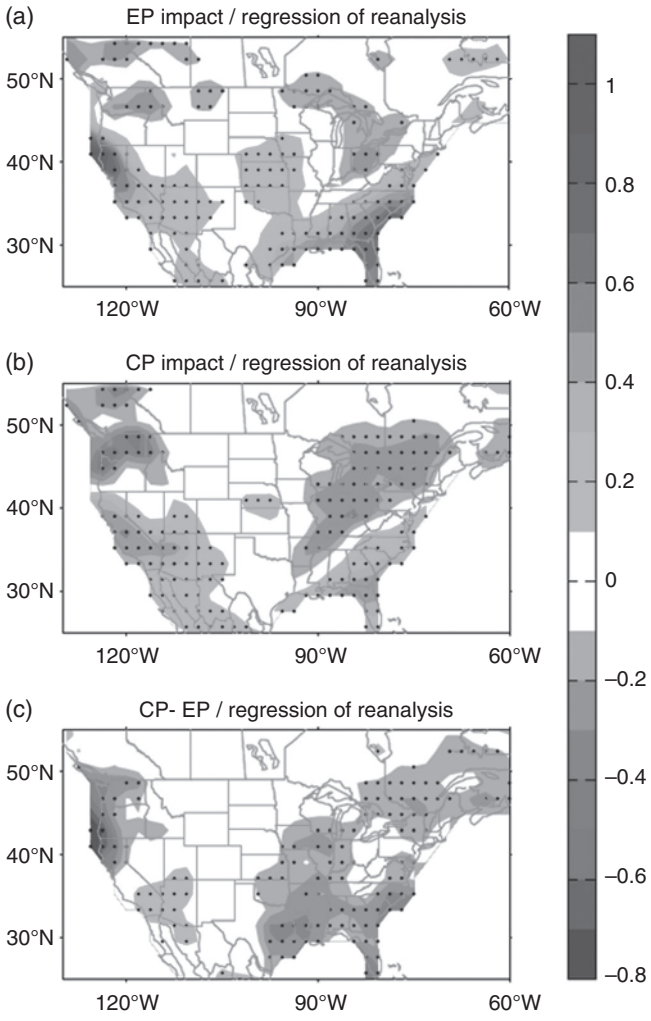

Figure 1.10 US winter (January–March) precipitation anomalies associated with (a) the EP El Niño and (b) the CP El Niño. The difference between the two types of El Niño (i.e., the CP impact minus EP impact) is shown in (c). The values shown are obtained by regressing US winter precipitation anomalies onto the EP and CP ENSO indices. Values shown are in units of mm/day, and the areas passing the 90% confidence level based on the Student's t-test are dotted. The NCEP/NCAR reanalysis dataset for the period of 1948–2010 is used. Adapted from *Yu and Zou* [2013].

The negative values in Figure 1.10c indicate that a shift in El Niño from the EP type to the CP type enhances the dry anomalies over the Pacific Northwest and along the Ohio-Mississippi valley and weakens the wet anomalies over the Southeast. As a result, the emerging CP El Niño produces an overall drying effect during the US winter. The different impacts on winter precipitation can lead to an asymmetric response between the two types of ENSO in the springtime soil water hydrology over the Mississippi River basin as shown by *Liang et al.* [2014], who also indicated that the winter to spring memory was carried through by subsurface hydrological storage processes.

Winter precipitation over the United States is primarily associated with winter storms, whose tracks are controlled by the locations of tropospheric jet streams. *Yu and Zou* [2013] related the enhanced drying effect of the CP ENSO to a more southward displacement of the tropospheric jet streams. Previous studies have suggested that such an equatorward shift of the tropospheric jet streams during El Niño events results from El Niño-induced Rossby wave trains and strengthening of the Hadley circulation [e.g., *Wang and Fu*, 2000; *Seager et al.,* 2003; *Lu et al.,* 2008]. As the jet streams shift southward, winter storms shift south as well, leading to a dry-north and wet-south pattern of precipitation anomalies during the El Niño. *Yu and Zou* [2013] found that the jet streams were displaced more southward during CP El Niño than during EP El Niño. The increased southward displacements of the jet streams cause dry anomalies over the northern United States (including the Northwest and Ohio-Mississippi valley), which expand and intensify more significantly during the CP El Niño than during the EP El Niño. Similarly, the wet anomalies over the southern United States expand over the Southwest and extend into Mexico during the CP El Niño. However, the same southward displacements over the East Coast push the core of the jet stream (and therefore the storm tracks) south of the US continent and into the Gulf of Mexico and the Caribbean, which results in only a small area of wet anomalies left in the southeast United States during the CP El Niño. One major implication of the findings of *Yu and Zou* [2013] is that the droughts occurring in the Ohio-Mississippi valley and Pacific Northwest during El Niño years may be intensified as El Niño becomes more frequently of the CP type and that the Southeast should not expect as much enhancement of winter precipitation during El Niño years as in the past. In addition to cold season impacts, *Liang et al.* [2015] suggested that the two ENSO types have different influences on the warm season (May–June) Great Plains low-level jet (GPLLJ) during their decaying phases. They found that the EP El Niño intensifies the GPLLJ while CP El Niño weakens the GPLLJ, the latter leading to drier conditions in the central United States.

Capotondi and Alexander [2010] have shown that CMIP3 models are capable of reproducing the general features of the observed precipitation pattern over North America despite the coarse resolutions of these global models. The six models they analyzed captured the observed precipitation maxima in the American Northwest and Southeast and the lower values in the central United States. Their analysis also showed that the seasonal cycles of precipitation produced by the CMIP3 models in the Great Plains were realistic, with a rainy

season that starts in early summer and slowly winds down toward winter. *Mo* [2010] also showed that the CMIP3 simulations could be useful in identifying the CP and EP ENSO's impacts on US winter climate. A series of studies organized by the National Oceanic and Atmospheric Administration (NOAA) Modeling, Analysis, Predictions, and Projections (MAPP) Program's CMIP5 Task Force have also demonstrated that CMIP5 models are useful in understanding the climate over North America [*Sheffield et al.,* 2013a, 2013b, 2014; *Maloney et al.,* 2014]. These recent studies demonstrated that CMIP simulations were useful for studying the regional climate impacts produced by global-scale climate phenomena. The performance of coupled climate models in simulating the EP and CP types of ENSO was also examined for both the CMIP3 models [*Yu and Kim*, 2010a] and the CMIP5 models [*Kim and Yu,* 2012]. Compared to the CMIP3 models, the CMIP5 models are found to better simulate the observed spatial patterns of the two types of ENSO and to have a significantly smaller intermodel diversity in ENSO intensity. The improved performance of the CMIP5 models is particularly apparent in the simulation of EP ENSO intensity, although it is still more difficult for the models to reproduce the observed EP ENSO intensity than the observed CP ENSO intensity. The performance of CMIP5 models in simulating the different impacts of the two types of ENSO on US winter climate was also examined in *Zou et al.* [2014], where 30 CMIP5 preindustrial simulations were examined to conclude that the CMIP5 models can simulate the observed EP El Niño impacts but not the observed CP El Niño impacts. The responses of observed US winter temperature to the EP El Niño are reasonably simulated by most of the CMIP5 models. The northeast-warm and southwest-cold pattern can be seen in many of the CMIP5 models. However, the observed northwest-warm and southeast-cold response pattern to the CP ENSO can only be found in some of the CMIP5 models. In some of the other CMIP5 models, the US winter temperature anomalies are even opposite from the observed.

Why are CMIP5 models less successful in simulating CP ENSO impact on the US winter climate? Heating associated with deep convection is a key process by which ENSO influences the atmosphere. The intensity and location of deep convection can be represented by the outgoing longwave radiation (OLR). The importance of using OLR anomalies to understand the atmospheric teleconnections from the tropics has been emphasized in many earlier studies [e.g., *Heddinghaus and Krueger*, 1981; *Lau and Chan*, 1983, 1985; *Gruber and Krueger*, 1984; *Ardanuy and Kyle*, 1986; *Chiodi and Harrison*, 2013]. *Zou et al.* [2014] looked into the relationships between SST and OLR anomalies for the two types of El Niño and examined how well the observed relationships were simulated in the CMIP5 models. It was found that during the EP ENSO, the strongest SST anomalies are located in the eastern equatorial Pacific and can easily influence the strength of the Walker circulation, giving rise to basinwide OLR anomalies. The modeled atmospheric responses to the EP El Niño are thus not sensitive to SST anomaly structure and can be well simulated by most of the CMIP5 models. In contrast, the SST anomalies of the CP El Niño are located in the central equatorial Pacific and can induce only local OLR anomalies to the west of the SST anomalies. The modeled atmospheric responses to the CP El Niño are, therefore, different among the models depending on the simulated magnitudes and locations of the CP El Niño SST anomalies. The finding reported by *Zou et al.* [2014] implies that it may become more challenging for climate models to simulate and predict ENSO's impacts on US climate as ENSO changes from the EP type to the CP type.

1.4.2. Western Pacific and Indian Oceans

ENSO events also produce significant impacts on the climate of the western Pacific and the Indian Ocean basin. In the conventional point of view, El Niño events shift tropical convection eastward to the equatorial central-to-eastern Pacific resulting in an anomalous Walker circulation that has an anomalous descending branch over the western Pacific, Maritime Continent, and northern Australia (Fig. 1.8a). This anomalous descending motion then induces two modes of Indian Ocean (IO) variability through surface heat fluxes and oceanic Rossby waves [e.g., *Klein et al.*, 1999; *Venzke et al.,* 2000; *Alexander et al.,* 2002; *Xie et al.,* 2002; *Yu* and Lau, 2004; *Yu et al.,* 2005; *Liu and Alexander*, 2007]. One of the modes is the Indian Ocean Dipole [*Saji et al.,* 1999; *Webster et al.,* 1999] that has one SST anomaly center in the tropical western Indian Ocean and the other center in the southeast Indian Ocean, and the other mode is the Indian Ocean basinwide warming (IOBW). The IOD tends to peak during El Niño's developing phase during autumn (September–November; SON) and IOBW peaks during El Niño's decaying phase during spring (March–May) [e.g., *Schott et al.,* 2009]. These ENSO-induced Indian Ocean variability modes are known to affect Indian summer monsoon, Australia and East Africa, the western North Pacific, and Southern Hemisphere high latitudes [e.g., *Saji et al.,* 1999; *Ashok et al.,* 2001, 2003; *Lau and Nath*, 2004; *Yang et al.,* 2007; *Xie et al.,* 2009]. Associated with the different Walker circulation response to two ENSO types (Fig. 1.8a and b), *Wang and Wang* [2014] suggested that the EP El Niño and some CP El Niño (El Niño Modoki I) events induce the positive IOD, while the other CP El Niño (El Niño Modoki II) events produce the negative

IOD. However, *Yu et al.* [2015b] argued that the EP El Niño events are more associated with the IOD while the CP El Niño events are not. *Paek et al.* [2015] showed that the EP El Niño events tend to be accompanied by basinwide warming in the Indian Ocean but not the CP El Niño events. The different Indian Ocean responses induced by the two types of ENSO bring different ENSO impacts to the neighboring regions. *Kumar et al.* [2006] used a historical rainfall record and AGCM experiments to suggest that the CP El Niño is more effective in enhancing subsidence over the Indian subcontinent during Indian summer monsoon season (June–September) leading to more severe droughts than during EP El Niños. *Yadav et al.* [2013] found that the EP El Niño leads to more precipitation over the north and central India regions during El Niño peak season (December–February). *Ratman et al.* [2014] reported significant drought in austral summer over southern Africa during EP El Niños but not during CP El Niños. Significant decreases in rainfall in Australia have been reported during CP El Niño events compared to the EP El Niño events [*Wang and Hendon*, 2007; *Lim et al.,* 2009; *Taschetto and England*, 2009].

1.4.3. East Asia

ENSO has profound impacts on East Asian climate variability such as the East Asian monsoon [e.g., *Zhang et al.,* 1999; *Chang et al.,* 2000; *Zhou and Chan*, 2007; *Li and Yang*, 2010], East Asian rainfall [e.g., *McBride et al.,* 2003; *Juneng and Tangang*, 2005; *Zhou et al.,* 2009], western Pacific tropical cyclone (TC) activity [e.g., *Chan*, 2000; *Chia and Ropelewski*, 2002; *Camargo and Sobel*, 2005; *Ho et al.,* 2004], and SSTs over the South China Sea [e.g., *He and Guan*, 1997; *Xie et al.,* 2003; *Wang et al.,* 2006; *Zhang et al.,* 2010]. The anomalous western North Pacific subtropical high (WNPSH) or low-level Philippine Sea anticyclone is a potentially important atmospheric component connecting ENSO and East Asian climate as suggested by several authors [e.g., *Zhang et al.,* 1999; *Wang et al.,* 2000; *Lau and Nath*, 2006; *Chou et al.,* 2009]. ENSO induces SST anomalies in the western Pacific to initiate the WNPSH during the ENSO developing seasons and the WNPSH variability is sustained until the following summer (June–August) through local air-sea interactions [*Wang et al.,* 2000], or the IO SST anomalies (i.e., IOBW) to excite a Kelvin wave to the east maintaining the WNPSH variability [*Yang et al.,* 2007; *Xie et al.,* 2009], or the tropical central Pacific SST anomalies that produce the WNPSH as a Rossby wave response to the west of the SST anomalies [*B. Wang et al.,* 2013], or the SST anomalies over the maritime continent that give rise to a local Hadley circulation descending into the WNPSH region [*Sui et al.,* 2007].

Recently, *Zhang et al.* [2011] contrasted the different impacts of the two ENSO types on the WNPSH. They found that during the El Niño developing phase in autumn, an intensified WNPSH for the EP El Niño but a weakened WNPSH for the CP El Niño. *Yuan et al.* [2012] further documented that from the El Niño developing summer to decaying summer, the EP El Niño is accompanied by a strong WNPSH that extends from the Indian Ocean to the east of the Philippines, while the CP El Niño is accompanied by a weak, short-lived WNPSH that is confined to the west of the Philippines. They also argued that the IO SST anomalies are responsible for the persistence of WNPSH into the ENSO following summer for the EP El Niño, but not for the CP El Niño. *Paek et al.* [2015] suggested in their observational and AGCM study, that the 3–5-yr band of summer WNPSH variability is more related to the EP ENSO and its SST anomalies over the Indian Ocean, whereas the 2–3-yr band of WNPSH variability is related to CP ENSO and its SST anomalies in the central Pacific and maritime continent. These different WNPSH responses to the two ENSO types are then shown to modulate East Asian climate. For example, southern China experiences increased rainfall during the EP El Niño but decreased rainfall during the CP El Niño due to the different WNPSH response and associated moisture transport into the region in El Niño developing phase in autumn [*Zhang et al.,* 2011], mature phase in winter [*Weng et al.,* 2009], and decaying phase in spring [*Feng and Li,* 2011]. During El Niño decay in summer, *Feng et al.* [2011] found increased rainfall south to the Yangtze River and decreased rainfall in the northern Yangtze–Huaihe river region for the EP El Niño, and increased rainfall in the Huaihe River–Yellow River region and decreased rainfall in southern China for the CP El Niño. *J.-S. Kim et al.* [2012] showed a significant increase in precipitation over South Korea and southern Japan during the CP El Niño that represents conditions opposite of those found for the EP El Niño. *Weng et al.* [2007] and *Yuan and Yang* [2012] also found that the different WNPSH can exert a different impact on the summer and winter monsoon over East and Southeast Asia, which implies difficulty in predicting East Asian monsoon variability based on the conventional monsoon-ENSO relationships [e.g., *Yang and Jiang*, 2014]. The WNPSH and associated convection also modulate TC activity over the South China Sea and western North Pacific during the El Niño developing phase in summer and autumn. The CP El Niño tends to enhance TC activity in the regions but the EP El Niño suppresses TC activity, which increases the TC landfall in Taiwan, South China, Korea, and Japan particularly in autumn [*Chen and Tam*, 2010; *Chen*, 2011; *Hong et al.,* 2011; *Kim et al.,* 2011; *Wang et al.,* 2014]. In the South China Sea, anomalous net surface heat flux associated with the different

atmospheric circulation responses to the two ENSO types leads to a strong warm basin mode during the EP El Niño and a warm semibasin mode during the CP El Niño [*Liu et al.,* 2014].

1.4.4. Europe and the Atlantic Ocean

ENSO can influence the Atlantic/European sector via the tropospheric temperature mechanism [*Chiang and Sobel,* 2002] and the atmospheric bridge mechanism [*Klein et al.,* 1999]. The tropospheric temperature mechanism involves an ENSO-induced tropical tropospheric warming that spreads to the Atlantic as a Kelvin wave response to ENSO forcing, which then increases SST anomalies there [e.g., *Yulaeva and Wallace,* 1994; *Enfield and Mayer,* 1997; *Chiang and Sobel*, 2002]. In the atmospheric bridge mechanism, ENSO weakens the Walker circulation and excites a PNA teleconnection pattern that reduces trade wind and evaporation in the tropical North Atlantic, leading to a warming there [e.g., *Lau and Nath*, 2004; *Klein et al.,* 1999; *Alexander et al.,* 2002]. The canonical El Niño is known to suppress Atlantic TC activity through changes in vertical wind shear over the main TC development region [e.g., *Gray*, 1984; *Goldenberg and Shapiro,* 1996] and changes in tropospheric and surface temperatures [*Tang and Neelin,* 2004]. Recently, *Kim et al.* [2009] found that in contrast to the EP El Niño, the CP El Niño tends to enhance Atlantic TC activity and increase landfall potential along the coast of the Gulf of Mexico and Central America, which is associated with the different impacts on the vertical wind shear in the main TC development region by the two ENSO types. In contrast, *S.-K. Lee et al.* [2010] and *Larson et al.* [2012] suggested that the CP El Niño has an insubstantial impact on Atlantic TC activity, which is associated with a weak warming of the tropical North Atlantic during the CP El Niño and a strong warming during the EP El Niño [*Rodrigues et al.,* 2011; *Amaya and Foltz*, 2014]. *Graf and Zanchettin* [2012] found different impacts on European winter temperatures. They showed that EP El Niño events lead to weak warming while CP El Niño events lead to significant cooling. They further attributed the European cooling to the negative phase of North Atlantic Oscillation (NAO) through the CP ENSO-NAO teleconnection in the troposphere.

1.4.5. Arctic

For the Northern Hemisphere high-latitude and Arctic climate, the ENSO signal can be transmitted there via a stratospheric pathway. Canonical El Niño events tend to be accompanied by a weakened Northern Hemisphere polar vortex. The positive PNA pattern and a deepened Aleutian low in the troposphere during El Niño may enhance planetary wave activities and increase the upward propagation of the waves into the stratosphere [e.g., *Garfinkel and Hartmann,* 2008; *Garfinkel et al.,* 2010; *Nishii et al.,* 2010], where they dissipate and result in a weakened polar vortex and more frequent polar stratospheric warmings [e.g., *Sassi et al.,* 2004; *García-Herrera et al.,* 2006; *Manzini et al.,* 2006]. The warm anomalies then descend to the troposphere in boreal winter through wave–mean flow interactions [e.g., *Holton*, 1976; *McIntyre,* 1982; *Zhou et al.,* 2002; *Manzini et al.,* 2006]. This weakened polar vortex and descending warm anomalies excite the Arctic Oscillation (AO) and the NAO [e.g., *Thompson and Wallace,* 1998; *Baldwin and Dunkerton*, 1999; *Zhou et al.,* 2002; *Kunz et al.,* 2009]. Recently, differing polar teleconnections between the two types of ENSO have been reported. *Hegyi and Deng* [2011] used post-1979 observations to suggest that in contrast to the EP El Niño, the CP El Niño can lead to a stronger polar vortex and a positive phase of the AO. They argued that the positive AO tendency associated with the CP El Niño events in recent decades has contributed to decadal changes in the Arctic precipitation. *Xie et al.* [2012] also reported a weakened midlatitude upward propagation of wave activity during the 1979–2010 CP El Niños, leading to a stronger and colder polar vortex. In contrast, *Graf and Zanchettin* [2012] showed both types of El Niño since 1948 were accompanied by a weakened polar vortex. *Zubiaurre and Calvo* [2012] and *Sung et al.* [2014] found a polar response (that is not statistically significant) to the CP El Niño that is related to a delayed deepening of the Aleutian low and weakened upward wave propagation to stratosphere. *Garfinkel et al.* [2013] compared the different composites used in previous studies [*Hegyi and Deng*, 2011; *Graf and Zanchettin*, 2012; *Xie et al.,* 2012; *Zubiaurre and Calvo*, 2012] to show that the diverse CP ENSO-Arctic teleconnections are very sensitive to the selection of CP El Niño events from the short observational record. *Iza and Calvo* [2015] emphasized the role of stratospheric sudden warming (SSW) events for the downward propagation. They found that with the SSWs removed, the different EP and CP El Niño responses are robust regardless of the CP El Niño definition and the composite size. In a modeling study, *Xie et al.* [2012] showed that whether the CP El Niño induces a strengthened or a weakened vortex depends on the phase of the quasi-biennial oscillation (QBO), while other studies [*Garfinkel et al.,* 2013; *Hurwitz et al.,* 2013; *Hurwitz et al.,* 2014] found a consistent weakening of the polar vortex under CP Niño SST forcing using a single AGCM. In the CMIP5 multimodel simulations, *Hurwitz et al.* [2014] found that the multimodel means show a weakening of the polar vortex during the EP El Niño in boreal winter, and a nonsignificant strengthening of the vortex during the CP El Niño.

1.4.6. Antarctica

In the Southern Hemisphere, ENSO has been suggested to influence mid-to-high-latitude climate [e.g., *Karoly*, 1989; *Mo*, 2000; *Yuan*, 2004], often via the two leading Southern Hemisphere atmospheric variability modes: the southern annular mode (SAM) [*Hartmann and Lo*, 1998; *Thompson and Wallace,* 2000] and the Pacific–South American teleconnection (PSA) [*Mo and Ghil*, 1987] pattern. For example, previous studies found that ENSO, together with the SAM and PSA, influenced South American rainfall [e.g., *Ropelewski and Halpert,* 1987, 1989; *Grimm*, 2003], the Southern Ocean SSTs [e.g., *Ciasto and Thompson,* 2008; *Yeo and Kim*, 2015], Antarctic sea-ice concentrations [e.g., *Liu et al.,* 2004; *Stammerjohn et al.,* 2008; *Yuan and Li,* 2008], and Antarctic surface air temperatures [e.g., *Kwok and Comiso,* 2002; *Ding et al.,* 2011; *Schneider et al.,* 2012]. Recently, several studies have begun to examine the different impacts of the two types of ENSO on the Southern Hemisphere climate. The westward shift of tropical Pacific convection during the CP El Niño can excite Rossby wave train (i.e., PSA) toward higher latitudes, which then results in suppressed storm track activity over Australia and enhanced activity over central Argentina [*Ashok et al.,* 2009], a northward displacement of the South American precipitation pattern [*Hill et al.,* 2009], the melting of Antarctic ice by inducing a stationary anticyclone and enhancing the eddy heat flux into the region [*T. Lee et al.,* 2010], and stronger Antarctic sea-ice variability [*Song et al.,* 2011]. In addition to the PSA pattern, early studies showed that the ENSO signals can be transmitted to high latitudes through a tropospheric pathway mechanism in which an ENSO-induced equatorward shift in the subtropical jet can change the midlatitude eddy activity and its associated eddy–mean flow interactions to modulate the SAM [e.g., *Seager et al.,* 2003; *L'Heureux and Thompson*, 2006; *Lu et al.,* 2008; *Chen et al.,* 2008]. Recent studies have used observations and GCM experiments to also suggest a stratospheric pathway mechanism in which the CP ENSO can affect the upward propagation of planetary waves into the stratosphere and induce polar temperature and vortex anomalies that subsequently descend into the troposphere to excite the SAM [e.g., *Mechoso et al.,* 1985; *Hurwitz et al.,* 2011a,b; *Lin et al.,* 2012; *Zubiaurre and Calvo,* 2012; *Son et al.,* 2013; *Evtushevsky et al.,* 2014].

Fogt and Bromwich [2006] noticed that the relationships among ENSO, PSA, and SAM can change from decade to decade, which is attributed to the strengthened ENSO–Southern Hemisphere influences from the 1980s to the 1990s. More recently, *Yu et al.* [2015b] further suggested a shift in the ENSO–Southern Hemisphere teleconnections occurred in the early 1990s. They conducted a 15 yr running correlation analysis among the SAM, PSA, and ENSO indices during austral spring (SON) for the period 1948–2014. For an ENSO index, they used cold tongue index (CTI; SST anomalies averaged over 6°S–6°N and 180°–90°W). They found that the correlation coefficient between the CTI and SAM index (Fig. 1.11e) dramatically increased from insignificantly small to significantly large values after the early 1990s, while the CTI-PSA correlation (Fig. 1.11f) stayed at significant values throughout the analysis period. The SST anomaly pattern correlated with the SAM or PSA index after the early 1990s is shown to be similar to the CP ENSO-SST anomaly pattern [*Kao and Yu,,* 2009], whereas the SST anomaly pattern correlated with the PSA index before the early 1990s is more similar to the pattern for the EP ENSO. Their composite analyses also showed both types of ENSO (Fig. 11a and b) can excite the PSA (Fig. 1.11d) while only CP type can excite the SAM (Fig. 1.11c) through tropospheric and stratospheric pathway mechanisms. The EP ENSO is found to induce the Indian Ocean Dipole but not the CP ENSO (Fig. 1.11a and b). *Yu et al.* [2015b] showed that the different influences of the two types of ENSO on the Indian Ocean SST anomalies enable these two ENSO types to produce difference influences on the SAM through eddy–mean flow interactions. They further suggested that the different ENSO–Southern Hemisphere teleconnections and more frequent occurrence of the CP ENSO in recent decades have led to a more in-phase SAM-PSA relationship after the early 1990s, which consequently impacted the post-1990s Antarctic climate in some aspects: an increase in the geopotential height anomalies over the Amundsen-Bellingshausen seas, a stronger Antarctic sea-ice dipole structure [e.g., *Yuan and Martinson*, 2001] between the Ross Sea and Weddell Sea, and a shift in the phase relationships of surface air temperature anomalies among the Antarctic Peninsula, East and West Antarctica. The findings of *Yu et al.* [2015b] imply that the linkages between ENSO and Antarctic climate depend on the dominant ENSO type and have become tighter during the recent two decades and will likely remain so in the coming decades if the dominance of the CP ENSO persists.

1.5. ENSO IN THE FUTURE

The changes in ENSO in the future warmer world are one major concern of the climate research community due to the profound impacts produced by ENSO. Climate models are generally used in ENSO projections; however, the behavior of ENSO differs strongly from model to model and is thus highly uncertain. Despite a number of studies, there is still no consensus on how ENSO SST variability will change in response to global warming [i.e., *Meehl et al.,* 1993; *Knutson et al.,* 1997; *Collins*, 2000b;

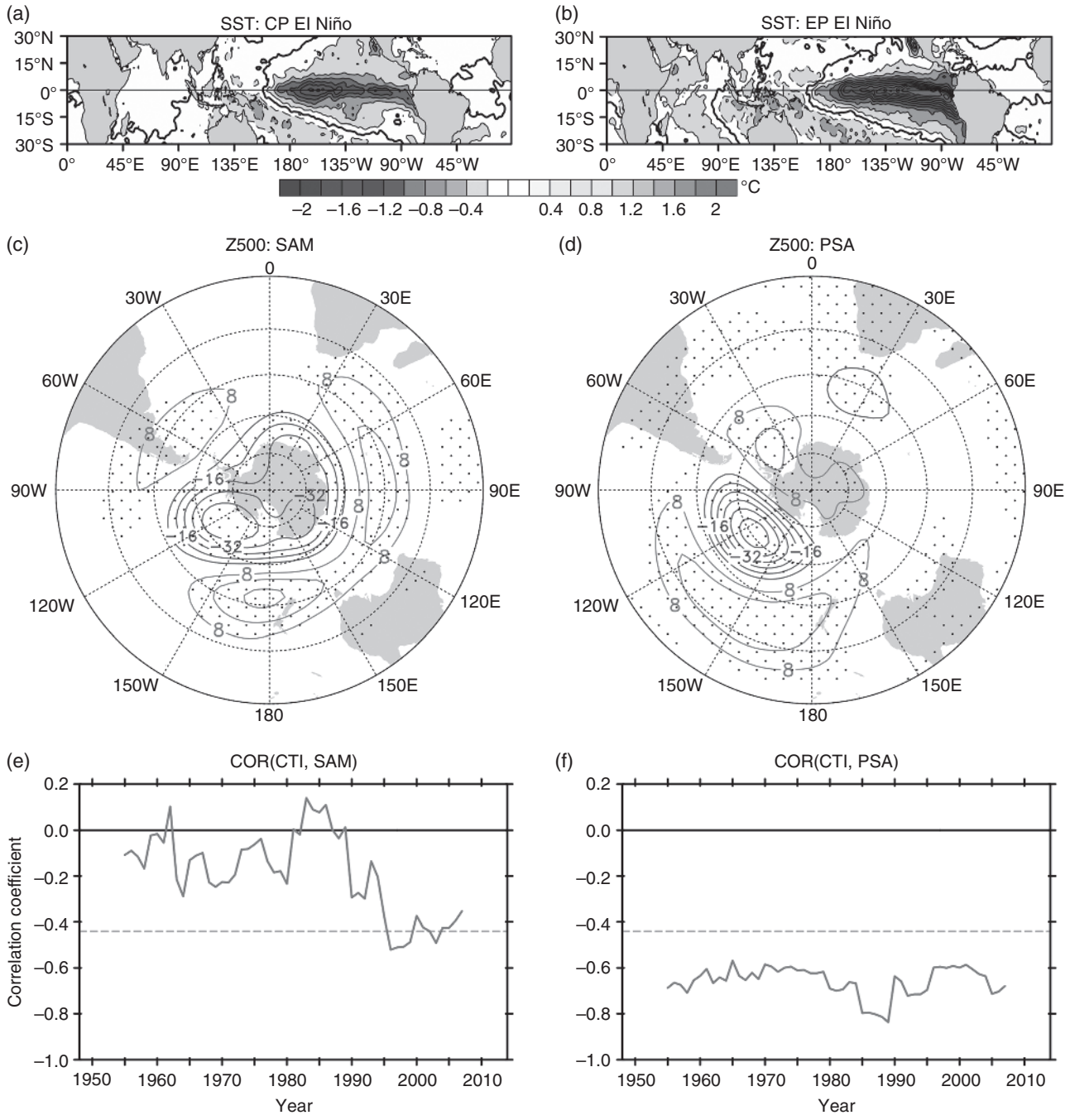

Figure 1.11 Upper panels show the composite SST anomalies for the (a) CP El Niño and (b) EP El Niño events during austral spring (SON). Middle panels show the 500 hPa geopotential height (Z500) anomaly structures of the (c) SAM and (d) PSA. Dots indicate areas where the values exceed the 95% confidence interval using a two-tailed Student's t-test. Contour interval is 8 m. Lower panels show the 15 yr running correlation coefficients (e) between the cold tongue index (CTI) and SAM index, and (f) between the CTI and PSA index. The green lines indicate the 90% confidence interval using a two-tailed Student's t-test. Modified from *Yu et al.* [2015b].

Zelle et al., 2005; *Guilyardi,* 2006; *Merryfield*, 2006; *An et al.,* 2008; *Yeh et al.,* 2009; *Newman et al.,* 2011; *Kim and Yu,* 2012; *Hu et al.,* 2012a; *Stevenson*, 2012; *Kim et al.,* 2014; *Cai et al.,* 2014; *L. Chen et al.,* 2015]. Model projections have yet to be conclusive on whether ENSO activity will be enhanced, weakened, or remain the same. The uncertainties come at least from three sources. The first source is related to the diverse abilities of climate models

to represent the physical processes responsible for determining the characteristics of ENSO. The second source comes from the different model projections of how the mean state may change under warming scenarios, which can modulate the strengths of the atmosphere-ocean feedbacks that characterize ENSO activity [e.g., *Collins*, 2000a, b]. The third source of uncertainty is related to the fact that intrinsic ENSO modulation can occur on interdecadal or intercentennial timescales even without external forcing [e.g., *Wittenberg*, 2009], which makes it difficult to determine if the ENSO changes produced in model projections are really global-warming related.

Early studies analyzing ENSO behavior in response to increasing greenhouse gas (GHG) were mostly based on a single CGCM [*Meehl et al.,* 1993; *Tett*, 1995; *Knutson et al.,* 1997; *Timmermann et al.,* 1999; *Collins*, 2000a, b; *Zelle et al.,* 2005]. For example, *Meehl et al.* [1993] used a CGCM with a coarse horizontal resolution to indicate little change in ENSO amplitude or period as the global atmosphere warms. A similar conclusion was obtained by *Tett* [1995] using a different climate model. *Knutson et al.* [1997] suggested that the responses of ENSO to global warming in models can depend on the model resolution. In coarse-resolution models, the impact of increased GHG on ENSO is unlikely to be clearly distinguishable from the climate system "noise" in the near future. *Timmermann et al.* [1999] used a model with a horizontal resolution high enough to adequately reproduce the narrow upwelling and low-frequency waves on the equator to suggest that ENSO events will become more frequent, stronger, and skew toward the La Niña phase as warming progresses. By comparing the ENSO behaviors under an identical 4 x CO2 scenario using two versions of the Hadley Centre coupled model, *Collins* [2000a] found significant changes in ENSO amplitude, frequency, and phase locking to the seasonal cycle in one version but not in the other version. Such discriminations are attributed to the differences in the mean pattern of climate change brought about by subtle changes in the physical parameterization between the two versions of the model. *Collins* [2000a], therefore, suggested that the uncertainties in the projection of future ENSO behavior also come from the model projections of the future mean climate states. The tropical Pacific mean state was projected to become more El Niño-like (i.e., with greater warming in the east than in the west) [e.g., *Meehl and Washington,* 1996; *Timmermann et al.,* 1999], more La Niña-like [e.g., *Noda et al.,* 1999], or uniformly warm [e.g., *Meehl et al.,* 2000] by various models, each of which may give rise to different changes in ENSO. In addition to the mean background SST state and its zonal gradient, the vertical contrast between the mean surface and subsurface temperatures (i.e., the upper ocean stratification) in the tropical Pacific is another mean state variable of crucial importance in determining future ENSO changes [*An et al.,* 2008].

To reduce the uncertainty related to the diverse model dynamics and physics, multimodel ensembles have been increasingly used for ENSO projections in recent years. This is particularly so after the CMIP3 and CMIP5 multimodel outputs were made available to the research community and were analyzed for the Intergovernmental Panel on Climate Change (IPCC) Assessment Reports. Among the studies that analyzed the CMIP3 models, *van Oldenborgh et al.* [2005] suggested that there are no statistically significant changes in the amplitude of ENSO variability in the projections. *Guilyardi* [2006] found that models capable of realistically simulating SST-wind feedback tend to project a significant increase in ENSO amplitude under elevated CO_2. In contrast to the change in ENSO amplitude, there were no clear indications of an El Niño frequency change. *Merryfield* [2006] suggested that changes in ENSO amplitude under CO_2 doubling are associated with the meridional width of the zonal wind stress response to ENSO in models. The models were found to have a 5% decrease in ENSO periods, which he argued resulted from an increase in equatorial wave speed through an associated speedup of the delayed-oscillator feedback. *Yeh and Kirtman* [2007] suggested that whether the model ENSO is in the linear or nonlinear regime determines the changes in ENSO statistics among various climate change projections.

Although the CMIP5 models represent an improvement over the CMIP3 models in many aspects (i.e., resolution, physics, etc.), the response of ENSO to global warming as seen in the CMIP5 output has not resolved this issue. The response of ENSO amplitude to global warming in CMIP5 shows great diversity from model to model, which is similar to that found in the CMIP3 models [*L. Chen et al.,* 2015]. Many studies found no consistent changes across the CMIP5 projections in the location, magnitude, frequency, or temporal evolution of ENSO events [*Stevenson*, 2012; *Taschetto et al.,* 2014]. *An and Choi* [2015] suggested that the feedback between ENSO and tropical climate change induced by global warming is very weak, which may be the reason why the global warming trend cannot significantly modify ENSO amplitude. Other CMIP5 studies have shown that greenhouse warming can alter both the amplitude of ENSO [*Kim et al.,* 2014] and the frequency of extreme ENSO events [*Cai et al.,* 2014, 2015]. *Kim et al.* [2014] analyzed the nine CMIP5 CGCMs that best reproduce the observed Bjerknes coupled stability index to project that, under global warming, ENSO amplitude is likely to increase after 2010, remain essentially unchanged until approximately 2040, and then decrease again afterward. *Cai et al.* [2014] suggested that global warming will increase the occurrence of extreme El Niño events, due to a faster warming in the eastern equatorial Pacific that enables

deep convection to occur more easily in the region and provide a coupled feedback to grow the ENSO amplitude. *Cai et al.* [2015] found an increased occurrence of extreme La Niña events under global warming due to an increased warming of the maritime continent compared to the equatorial central Pacific that enables convection to move to the maritime continent more easily to trigger the Bjerknes feedback favoring the extreme events.

After the recent recognition of different types of ENSO, how the ENSO type responds to future warming has also been explored in literature. Modeling studies have suggested that anthropogenic greenhouse gas forcing can be one of the causes for the increased occurrence of the CP El Niño [*Yeh et al.,* 2009; *Collins et al.,* 2010; *Na et al.,* 2011; *Kim and Yu,* 2012]. *Yeh et al.* [2009] used the CMIP3 models to suggest that the occurrence frequency of the CP ENSO will increase in the future, while *Kim and Yu,* [2012] used CMIP5 models to suggest the amplitude of CP ENSO will increase too. *Na et al.* [2011] projected that the occurrence frequency of the CP El Niño during 2007–2056 will be 2.5 times that in the 1980–2006 period.

In addition to the response of ENSO properties to global warming, changes in ENSO teleconnection under global warming scenarios have attracted substantial attention [i.e., *Meehl and Teng*, 2007; *Kug et al.,* 2010; *Zou et al.,* 2014]. Based on a six-member multimodel ensemble, *Meehl and Teng* [2007] identify some possible changes in the future El Niño teleconnections. Among them, the anomalous low in the North Pacific is suggested to weaken and shift eastward and northward in future events. This location shift may lead to a decreased anomalous warming over northern North America, increased cooling over southern North America, and enhanced precipitation in the Pacific Northwest compared to present-day El Niño event teleconnections. *Kug et al.* [2010] also found that the atmospheric teleconnection patterns over the Northern Hemisphere may shift eastward due to an eastward migration of the convection centers in the tropical Pacific associated with the future ENSO events. *Zou et al.* [2014] also found the ENSO-forced Pacific–North American teleconnection pattern to become stronger and more eastward displaced in the warming projections. These are just a few examples of possible ways that the changing ENSO may impact a future warmer world.

1.6. SUMMARY

The changing properties of the ENSO observed during the past two decades and the recent identification of two distinct types of ENSO have prompted the climate research community to revisit traditional views of ENSO dynamics and impacts and how they may change as global climate changes. A better understanding of ENSO diversity is important for the further development of models used for the prediction of ENSO and its associated climate extremes. One source of uncertainty in climate predictions and projections is associated with whether or not modern climate models can realistically simulate both types of ENSO and the alternation between them, and capture their different impacts. If ENSO dynamics are conclusively shown to be changing, the ENSO prediction models and strategies have to be revised to include this changing dynamic. For instance, successful prediction and modeling of the ENSO in the recent and coming decades may depend more on a better understanding and improved skill in the modeling of the subtropical Pacific precursors and their underlying generation mechanisms. Prediction systems based on this framework would be different from the prediction and modeling systems the climate research community has relied on since the 1980s and 1990s for the conventional ENSO that emphasize subsurface ocean dynamics in the equatorial Pacific. *Larson and Kirtman* [2014] have reported some skill in using the PMM to forecast ENSO events with the North American multimodel ensemble (NMME) experiments. *Yang and Jiang* [2014] showed that the National Centers for Environmental Prediction (NCEP) Climate Forecast System had substantial skill in predicting both types of ENSO and the relationship between the EP ENSO and the Asian monsoon. However, the skill in predicting the relationship between CP ENSO and the monsoon is low. Nevertheless, in order to utilize the subtropical precursors, particularly the PMM, to forecast ENSO events, coupled atmosphere-ocean models have to be able to realistically simulate the precursor events. *Lin et al.* [2014] examined 23 CMIP5 models to conclude that the PMM structure can be reasonably simulated in most of the coupled models. However, the so-called seasonal footprinting mechanism that sustains an equatorward extension of the PMM is not well simulated in a majority of the CMIP5 models. Therefore, it is necessary to improve the subtropical Pacific coupling in these models in order for them to apply them successfully in forecasts of ENSO occurrence. Currently, paleoclimate proxy records have mostly been interpreted from the point of view that there is a single type of ENSO (EP) and one set of conventional global impacts (such as precipitation) to derive the history of ENSO. The view that the two types of ENSO can produce distinct global teleconnection offers an additional way to interpret the paleoclimate proxies. A deeper understanding of how the changing El Niño affects global precipitation may also offer different ways to interpret paleoclimate proxies, which may lead to a new understanding of the history of Earth's climate and new implications for future climate changes.

ACKNOWLEDGMENTS

This work was supported by the National Science Foundation's Climate and Large Scale Dynamics Program (Grants AGS-1233542 and AGS-1505145), the National Key Research Program of China (Grant 2014CB953900), the National Oceanic and Atmospheric Administration's Modeling, Analysis, Predictions, and Projections Program (Grant NA11OAR4310102), and the National Natural Science Foundation of China (Grants 41422601, 41376025, 41690123 and 41690120).

REFERENCES

Alexander, M. A., and C. Deser (1995), A mechanism for the recurrence of wintertime midlatitude SST anomalies, *J. Phys. Oceanogr.*, *25*, 122–137.

Alexander, M. A., D. J. Vimont, P. Chang, and J. D. Scott (2010), The impact of extratropical atmospheric variability on ENSO: Testing the seasonal footprinting mechanism using coupled model experiments, *J. Climate*, *23*, 2885–2901; doi:10.1175/2010JCLI3205.1.

Alexander, M. A., I. Blade, M. Newman, J. R. Lanzante, N.-C. Lau, and J. D. Scott (2002), The atmospheric bridge: The influence of ENSO teleconnections on air-sea interaction over the global oceans, *J. Climate*, *15*, 2205–2231.

Amaya, D.J., and G.R. Foltz (2014), Impacts of canonical and Modoki El Niño on tropical Atlantic SST, *J. Geophys. Res. Oceans*, *119* (2), 777–789.

An, S.-I., and B. Wang (2000), Interdecadal change of the structure of ENSO mode and its impact on the ENSO frequency, *J. Climate*, *13*, 2044–2055.

An S.-I., and F.-F. Jin (2001), Collective role of zonal advective and thermocline feedbacks in ENSO mode, *J. Climate*, *14*, 3421–3432; doi: http://dx.doi.org/10.1175/1520-0442[2001]014<3421:CROTAZ>2.0.CO;2.

An, S.-I., and F.-F. Jin (2004), Nonlinearity and Asymmetry of ENSO, *J. Climate*, *17*, 2399–2412; doi: http://dx.doi.org/10.1175/1520-0442[2004]017<2399:NAAOE>2.0.CO;2.

An, S-I., and J. Choi (2015), Why the twenty-first century tropical Pacific trend pattern cannot significantly influence ENSO amplitude? *Climate Dyn.*, *44* (1–2), 133–146.

An, S.-I., J.-S. Kug, Y.-G. Ham, and I.-S. Kang (2008), Successive modulation of ENSO to the future greenhouse warming, *J. Climate*, *21*, 3–21.

Anderson, B. T. (2004), Investigation of a large-scale mode of ocean atmosphere variability and its relation to tropical Pacific sea surface temperature anomalies, *J. Climate*, *17*, 1089–4098; doi: 10.1175/1520-0442[2004]017<4089:IOALMO>2.0.CO;2.

Ardanuy, P. E., and H. L. Kyle (1986), Observed perturbations of the Earth's radiation budget: A response to the El Chichón stratospheric aerosol layer?, *J. Climate Appl. Meteor.*, *25*, 505–516; doi:10.1175/1520-0450[1986]025<0505:OPOTER>2.0.CO;2.

Ashok, K., C. Tam, and W. Lee (2009), ENSO Modoki impact on the Southern Hemisphere storm track activity during extended austral winter, *Geophys. Res. Lett.*, *36*, L12705; doi:10.1029/2009GL038847.

Ashok, K., Z. Gaun, and T. Yamagata (2001), Impact of the Indian ocean dipole on the relationship between the Indian monsoon rainfall and ENSO, *Geophys. Res. Lett.*, *28*, 4459–4502.

Ashok, K., Z. Gaun, and T. Yamagata (2003), Impact of the Indian Ocean dipole on the Australian winter rainfall. *Geophys. Res. Lett.*, *30*, 1821; doi:10.1029/2003GL017926.

Ashok, K., S. K. Behera, S. A. Rao, H. Weng, and T. Yamagata (2007), El Niño Modoki and its possible teleconnection, *J. Geophys. Res.*, *112*, C11007; doi:10.1029/2006JC003798.

Baldwin, M. P., and T. J. Dunkerton (1999), Propagation of the Arctic Oscillation from the stratosphere to the troposphere, *J. Geophys. Res.*, *104*, 30937–30946; doi:10.1029/1999JD900445.

Barnett, T. P. (1991), The interaction of multiple time scales in the tropical climate system, *J. Climate*, *4*, 269–285; doi: http://dx.doi.org/10.1175/1520-0442[1991]004<0269:TIOMTS>2.0.CO;2.

Barnett, T. P., D. W. Pierce, M. Latif, D. Dommenget, and R. Saravanan (1999), Interdecadal interactions between the tropics and midlatitudes in the Pacific basin, *Geophys. Res. Lett.*, *26*, 615–618.

Barnston, A. G., M. K. Tippett, M. L. L'Heureux, S. Li, and D. G. DeWitt (2012), Skill of real-time seasonal ENSO model predictions during 2002–11: Is our capability increasing?, *Bull. Amer. Meteor. Soc.*, *93*, 631–651.

Barsugli, J. J., and P. D. Sardeshmukh (2002), Global atmospheric sensitivity to tropical SST anomalies throughout the Indo-Pacific basin, *J. Climate*, *15*, 3427–3442.

Battisti, D. S., and A. C. Hirst (1989), Interannual variability in the tropical atmosphere-ocean model: Influence of the basic state, ocean geometry and nonlinearity, *J. Atmos. Sci.*, *45*, 1687–1712; doi:10.1175/1520-0469%281989%29046<1687%3AIVIATA>2.0.CO%3B2.

Behera, S. K., and T. Yamagata (2003), Influence of the Indian Ocean dipole on the Southern Oscillation, *J. Meteor. Soc. Japan*, *81*, 169–177.

Bjerknes, J. (1969), Atmospheric teleconnections from the equatorial Pacific, *Monthly Weather Rev.*, *97*, 163–172; doi: http://dx.doi.org/10.1175/1520-0493[1969]097<0163:ATFTEP>2.3.CO;2.

Cai, W., G. Wang, A. Santoso, M. J. McPhaden, L. Wu, F.-F. Jin, A. Timmermann, M. Collins, G. Vecchi, M. Lengaigne, M. H. England, D. Dommenget, K. Takahashi, and E. Guilyardi (2015), Increased frequency of extreme La Niña events under greenhouse warming, *Nature Climate Change*, *5*, 132–137; doi:10.1038/nclimate2492.

Cai, W., S. Borlace, M. Lengaigne, P. van Rensch, M. Collins, G. Vecchi, A. Timmermann, A. Santoso, M. J. McPhaden, L. Wu, M. H. England, G. Wang, E. Guilyardi, and Fei-Fei Jin (2014), Increasing frequency of extreme El Niño events due to greenhouse warming. *Nature Climate Change*, *4*, 111–116; doi: 10.1038/nclimate2100.

Camargo, S. J., and A. H. Sobel (2005), Western North Pacific tropical cyclone intensity and ENSO, *J. Climate*, *18*, 2996–3006.

Capotondi, A., and M. A. Alexander (2010), Relationship between precipitation in the Great Plains of the United States and global SSTs: Insights from the IPCC-AR4 models, *J. Climate*, *23*, 2941–2958.

Capotondi, A., A. T. Wittenberg, M. Newman, E. Di Lorenzo, J.-Y. Yu, P. Braconnot, J. Cole, B. Dewitte, B. Giese, E. Guilyardi, F.-F. Jin, K. Karnauskas, B. Kirtman, T. Lee, N. Schneider, Y. Xue, and S.-W. Yeh (2015), Understanding ENSO diversity, *Bull. Amer. Meteor. Soc.*; doi:10.1175/BAMS-D-13-00117.1.

Carton, J. A., G. A. Chepurin, X. Cao, and B. S. Giese (2000), A simple ocean data assimilation analysis of the global upper ocean 1950–1995, Part I: Methodology, *J. Phys. Oceanogr.*, *30*, 294–309; doi:10.1175/1520-0485[2000]030<0294:ASODA A>2.0.CO;2.

Cayan, D. R., K. T. Redmond, and L. G. Riddle, 1999), ENSO and hydrologic extremes in the western United States, *J. Climate*, *12*, 2881–2893.

Chan, J. C. L. (2000), Tropical cyclone activity over the western North Pacific associated with El Niño and La Niña events, *J. Climate*, *13*, 2960–2972.

Chang, C. P., Y. Zhang, and T. Li (2000), Interannual and interdecadal variations of the East Asian summer monsoon and tropical Pacific SSTs, Part I: Roles of the subtropical ridge, *J. Climate*, *13*, 4310–4325.

Chang, P., B. S. Giese, L. Ji, H. F. Seidel, and F. Wang (2001), Decadal change in the south tropical Pacific in a global assimilation analysis, *Geophys. Res. Lett.*, *28*, 3461–3464.

Chang, P., B. Wang, T. Li, and J. Lin (1995), Interactions between the seasonal cycle and El Niño–Southern Oscillation in an intermediate coupled ocean–atmosphere model, *J. Atmos. Sci.*, *52*, 2353–2372.

Chang, P., L. Ji, H. Li, and M. Flügel (1996), Chaotic dynamics versus stochastic processes in El Niño–Southern Oscillation in coupled ocean-atmosphere models, *Physica D: Nonlinear Phenomena*, *98* (2), 301–320.

Chang, P., L. Zhang, R. Saravanan, D. J. Vimont, J. C. H. Chiang, L. Ji, H. Seidel, and M. K. Tippett (2007), Pacific meridional mode and El Niño–Southern Oscillation, *Geophys. Res. Lett.*, *34*, L16608; doi:10.1029/2007GL030302.

Chen, D., T. Lian, C. Fu, M. A. Cane, Y. Tang, R. Murtugudde, X. Song, Q. Wu, and L. Zhou (2015), Strong influence of westerly wind bursts on El Niño diversity, *Nat. Geosci.*, *8* (5), 339–345.

Chen, G. (2011), How does shifting pacific ocean warming modulate on tropical cyclone frequency over the South China Sea?, *J. Climate*, *24*, 4695–4700.

Chen, G., and C.-Y. Tam (2010), Different impacts of two kinds of Pacific Ocean warming on tropical cyclone frequency over the western North Pacific, *Geophys. Res. Lett.*, *37*, L01803; doi:10.1029/2009GL041708.

Chen, G., J. Lu, and D. M. W. Frierson (2008), Phase speed spectra and the latitude of surface westerlies: Interannual variability and global warming trend, *J. Climate*, *21*, 5942–5959.

Chen, L., T. Li, and Y. Yu (2015), Causes of strengthening and weakening of ENSO amplitude under global warming in four CMIP5 models, *J. Climate*, *28*, 3250–3274; doi:10.1175/JCLI-D-14-00439.1.

Chia, H. H., and C. F. Ropelewski (2002), The interannual variability in the genesis location of tropical cyclones in the northwest Pacific, *J. Climate*, *15*, 2934–2944.

Chiang, J. C. H., and D. J. Vimont (2004), Analogous Pacific and Atlantic meridional modes of tropical atmosphere-ocean variability, *J. Climate*, *17*, 4143–4158; doi:10.1175/JCLI4953.1.

Chiang, J. C., and Sobel, A. H. (2002), Tropical tropospheric temperature variations caused by ENSO and their influence on the remote tropical climate, *J. Climate*, *15*, 2616–2631.

Chiodi, A. M., and D. E. Harrison (2013), El Niño impacts on seasonal U.S. Atmospheric circulation, temperature, and precipitation anomalies: The OLR-event perspective, *J. Climate*, *26*, 822–837; doi: http://dx.doi.org/10.1175/JCLI-D-12-00097.1.

Choi, J., S. -I. An, and S. W. Yeh (2012), Decadal amplitude modulation of two types of ENSO and its relationship with the mean state, *Climate Dyn.*, *38* (11–12), 2631–2644.

Choi, J., S. -I. An, B. Dewitte, and W. W. Hsieh (2009), Interactive feedback between the tropical Pacific Decadal Oscillation and ENSO in a coupled general circulation model, *J Climate*, *22*, 6597–6611.

Chou, C., L.-F. Huang, J.-Y. Tu, L. Tseng, and Y.-C. Hsueh (2009), El Niño impacts on precipitation in the western North Pacific–East Asian sector, *J. Climate*, *22*, 2039–2057.

Chung, P.-H., and T. Li (2013), Interdecadal relationship between the mean state and El Niño types, *J. Climate*, *26*, 361–379; doi:10.1175/JCLI-D-12-00106.1.

Ciasto, L. M., and D. W. J. Thompson (2008), Observations of large scale ocean-atmosphere interaction in the Southern Hemisphere, *J. Climate*, *21*, 1244–1259; doi:10.1175/2007JCLI1809.1.

Clement, A., P. DiNezio, and C. Deser (2011), Rethinking the ocean's role in the Southern Oscillation, *J. Climate*, *24*, 4056–4072; doi:10.1175/2011JCLI3973.1.

Collins, M. (2000a), Understanding uncertainties in the response of ENSO to greenhouse warming, *Geophys. Res. Lett.*, *27*, 3509–3513.

Collins, M. (2000b), The El Niño Southern Oscillation in the second Hadley centre coupled model and its response to greenhouse warming, *J. Climate*, *13*, 1299–1312.

Collins, M., and coauthors (2010), The impact of global warming on the tropical Pacific Ocean and El Niño, *Nat. Geosci.*, *3*, 391–397; doi:10.1038/NGEO868.

Cummins, P. F., G. S. E. Lagerloef, and G. Mitchum (2005), A regional index of northeast Pacific variability based on satellite altimeter data, *Geophys. Res. Lett.*, *32*, L17607; doi:10.1029/2005GL023642.

Dettinger, M. D., D. R. Cayan, H. F. Diaz, and D. M. Meko (1998), North-south precipitation patterns in western North America on interannual-to-decadal timescales, *J. Climate*, *11*, 3095–3111.

DeWeaver, E., and S. Nigam (2004), On the forcing of ENSO teleconnections by anomalous heating and cooling, *J. Climate*, *17*, 3225–3235.

Ding, Q., E. J. Steig, D. S. Battisti, and M. Kuettel (2011), Winter warming in West Antarctica caused by central tropical Pacific warming, *Nat. Geosci.*, *4*, 398–403; doi:10.1038/ngeo1129.

Dommenget, D. (2010), The slab ocean El Niño, *Geophys. Res. Lett.*, *37*, L20701; doi:10.1029/2010/GL044888.

Dong, B., R. T. Sutton, and A. A. Scaife (2006), Multidecadal modulation of El Niño–Southern Oscillation (ENSO) variance by Atlantic Ocean sea surface temperatures, *Geophys. Res. Lett.*, *33*, L08705; doi:10.1029/2006GL025766.

Dong, B. W., and R. Y. Lu (2013), Interdecadal enhancement of the Walker circulation over the tropical Pacific in the late 1990s, *Adv. Atmos. Sci.*, *30* (2), 247–262; doi: 10.1007/s00376-012-2069-9.

Duan, W., H. Xu, and M. Mu (2008), Decisive role of nonlinear temperature advection in El Niño and La Niña amplitude asymmetry, *J. Geophys. Res.*, *113*, C01014; doi:10.1029/2006JC003974.

Enfield, D. B., and D. A. Mayer (1997), Tropical Atlantic sea surface temperature variability and its relation to El Niño–Southern Oscillation, *J. Geophys. Res.*, *102*, 929–945; doi:10.1029/96JC03296.

England, M. H., S. McGregor, P. Spence, G. A. Meehl, A. Timmermann, W. Cai, A. S. Gupta, M. J. McPhaden, A. Purich, and A. Santoso (2014), Recent intensification of wind-driven circulation in the Pacific and the ongoing warming hiatus, *Nature Climate Change*, *4*, 222–227; doi:10.1038/nclimate2106.

Evtushevsky, O. M., V. O. Kravchenko, L. L. Hood, and G. P. Milinevsky (2014), Teleconnection between the central tropical Pacific and the Antarctic stratosphere: Spatial patterns and time lags, *Climate Dyn.*, 1–15.

Fedorov, A. V., and S. G. Philander (2000), Is El Niño changing?, *Science*, *288*, 1997–2002.

Fedorov, A. V., S. Hu, M. Lengaigne, and E. Guilyardi (2014), The impact of westerly wind bursts and ocean initial state on the development, and diversity of El Niño events, *Climate Dyn.*, *44* (5–6), 1381–1401.

Feng, J., and J. Li (2011), Influence of El Niño Modoki on spring rainfall over South China, *J. Geophys. Res.*, *116*, D13102; doi:10.1029/2010JD015160.

Feng, J., W. Chen, C.-Y. Tam, and W. Zhou (2011), Different impacts of El Niño and El Niño Modoki on China rainfall in the decaying phases, *Int. J. Climatol.*, *31*, 2091–2101; doi:10.1002/joc.2217.

Fogt, R. L., and D. H. Bromwich (2006), Decadal variability of the ENSO teleconnection to the high-latitude South Pacific governed by coupling with the southern annular mode, *J. Climate*, *19*, 979–997; doi:10.1175/JCLI3671.1.

Frauen, C., and D. Dommenget (2010), El Niño and La Niña amplitude asymmetry caused by atmospheric feedbacks, *Geophys. Res. Lett.*, *37*, L18801; doi:10.1029/2010GL044444.

Fu, C., H. F. Diaz, J. O. Fletcher (1986), Characteristics of the response of sea surface temperature in the central Pacific associated with warm episodes of the Southern Oscillation. *Monthly Weather Rev.*, *114*, 1716–1738.

García-Herrera, R., N. Calvo, R. R. Garcia, and M. A. Giorgetta (2006), Propagation of ENSO temperature signals into the middle atmosphere: A comparison of two general circulation models and ERA-40 reanalysis data, *J. Geophys. Res.*, *111*, D06101; doi:10.1029/2005JD006061.

Garfinkel, C. I., and D. L. Hartmann (2008), Different ENSO teleconnections and their effects on the stratospheric polar vortex, *J. Geophys. Res.*, *113*, D18114; doi:10.1029/2008JD009920.

Garfinkel, C. I., D. L. Hartmann, and F. Sassi (2010), Tropospheric precursors of anomalous Northern Hemisphere stratospheric polar vortices, *J. Climate*, *23*, 3282–3299; doi:10.1175/2010JCLI3010.1.

Garfinkel, C. I., M. M. Hurwitz, D. W. Waugh, and A. H. Butler (2013), Are the teleconnections of central Pacific and eastern Pacific El Niño distinct in boreal wintertime?, *Climate Dyn.*, *41*, 1835–1852; doi:10.1007/s00382-012-1570-2.

Goldenberg, S. B., and L. J. Shapiro (1996), Physical mechanisms for the association of El Niño and West African rainfall with Atlantic major hurricane activity, *J. Climate*, *9*, 1169–1187; doi:10.1175/1520-0442[1996] 009<1169:PMFTAO>2.0.CO;2.

Graf, H. F., and D. Zanchettin (2012), Central Pacific El Niño, the "subtropical bridge," and Eurasian climate, *J. Geophys. Res.*, *117*, D01102; doi:10.1029/2011JD016493.

Gray, W. M. (1984), Atlantic seasonal hurricane frequency. Part I: El Niño and 30-mb quasi-biennial oscillation influences. *Monthly Weather Rev.*, *112*, 1649–1668.

Grimm, A. M. (2003), The El Niño impact on the summer monsoon in Brazil: Regional processes versus remote influences, *J. Climate*, *16*, 263–280.

Gruber, A., and A. F. Krueger (1984), The status of the NOAA outgoing longwave radiation data set, *Bull. Amer. Meteor. Soc.*, *65*, 958–962; doi:10.1175/1520-0477[1984]065<0958:TSOTNO>2.0.CO;2.

Gu, D., and S. G. H. Philander (1995), Secular changes of annual and interannual variability in the tropics during the past century, *J. Climate*, *8*, 864–876; doi: http://dx.doi.org/10.1175/1520-0442[1995]008<0864:SCOAAI>2.0.CO;2.

Gu, D., and S. G. H. Philander (1997), Interdecadal climate fluctuations that depend on exchanges between the tropics and extratropics, *Science*, *275*, 805–807.

Guilyardi, E. (2006), El Niño-mean state-seasonal cycle interactions in a multi-model ensemble, *Climate Dyn.*, *26*, 329–348.

Hannachi, A., D. Stephenson, and K. Sperber (2003), Probability-based methods for quantifying nonlinearity in the ENSO, *Climate Dyn.*, *20*, 241–256.

Hartmann, D. L., and F. Lo (1998), Wave-driven zonal flow vacillation in the Southern Hemisphere, *J. Atmos. Sci.*, *55*(8), 1303–1315.

He, H., J. Yang, D. Gong, R. Mao, Y. Wang, and M. Gao (2015), Decadal changes in tropical cyclone activity over the western North Pacific in the late 1990s, *Climate Dyn.*, 1–13.

He, Y., and C. Guan (1997), Interannual and interdecadal variability in heat content of the upper ocean of South China Sea, *Adv. Atmos. Sci.*, *16*, 23–29.

Heddinghaus, T. R., and A. F. Krueger (1981), Annual and interannual variations in outgoing longwave radiation over the tropics, *Monthly Weather Rev., 109*, 1208–1218; doi: http://dx.doi.org/10.1175/1520-0493[1981]109<1208:AAIVIO>2.0.CO;2.

Hegyi, B. M., and Y. Deng (2011), A dynamical fingerprint of tropical Pacific sea surface temperatures on the decadal-scale variability of cool-season Arctic precipitation, *J. Geophys. Res.*, *116*, D20121; doi:10.1029/2011JD016001.

Hill, K. J., A. S. Taschetto, and M. H. England (2009), South American rainfall impacts associated with inter-El Niño variations, *Geophys. Res. Lett.*, *36*, L19702; doi:10.1029/2009GL040164.

Ho, C. H., J. J. Baik, J. H. Kim, D. Y. Gong, and C. H. Sui (2004), Interdecadal changes in summertime typhoon tracks, *J. Climate*, *17*, 1767–1776.

Hoerling, M. P., and A. Kumar (2002), Atmospheric response patterns associated with tropical forcing, *J. Climate*, *15*, 2184–2203.

Holton, J. R. (1976), A semi-spectral numerical model for wave-mean flow interactions in the stratosphere: applications to sudden stratospheric warmings, *J. Atmos. Sci.*, *33*, 1639–1649.

Hong, C.-C., Y.-H. Li, T. Li, and M.-Y. Lee (2011), Impacts of central Pacific and eastern Pacific El Nino on tropical cyclone tracks over the western North Pacific, *Geophys. Res. Lett.*, *38*, L16712; doi:10.1029/2011GL048821.

Horii, T., I. Ueki, and K. Hanawa (2012), Breakdown of ENSO predictors in the 2000s: Decadal changes of recharge/discharge-SST phase relation and atmospheric intraseasonal forcing, *Geophys. Res. Lett.*, *39*, L10707; doi:10.1029/2012GL051740.

Hsieh, W. W. (2004), Nonlinear multivariate and time series analysis by neural network methods, *Rev. Geophys.*, *42*, RG1003; doi:10.1029/2002RG000112.

Hu, S., A. V. Fedorov, M. Lengaigne, and E. Guilyardi (2014), The impact of westerly wind bursts on the diversity and predictability of El Niño events: an ocean energetics perspective. *Geophys. Res. Lett.*, *41*, 4654–4663; doi:10.1002/2013GL058954.

Hu, Z.-Z., A. Kumar, B. Jha, and B. Huang (2012a), An analysis of forced and internal variability in a warmer climate in CCSM3, *J. Climate*, *25* (7), 2356–2373; doi: 10.1175/JCLI-D-11-00323.1.

Hu, Z.-Z., A. Kumar, B. Jha, W. Wang, B. Huang, and B. Huang (2012b), An analysis of warm pool and cold tongue El Niños: Air-sea coupling processes, global influences, and recent trends, *Climate Dyn.*, *38* (9–10), 2017–2035; doi: 10.1007/s00382-011-1224-9.

Hu, Z.-Z., A. Kumar, H.-L. Ren, H. Wang, M. L'Heureux, and F.-F. Jin (2013), Weakened interannual variability in the tropical Pacific Ocean since 2000, *J. Climate*, *26* (8), 2601–2613; doi: 10.1175/JCLI-D-12-00265.1.

Huang, H. P., R. Seager, and Y. Kushnir (2005), The 1976/77 transition in precipitation over the Americas and the influence of tropical sea surface temperature, *Climate Dyn.*, *24* (7–8), 721–740.

Hurwitz, M. M., C. I. Garfinkel, P. A. Newman, and L. D. Oman (2013), Sensitivity of the atmospheric response to warm pool El Niño events to modeled SSTs and future climate forcings, *J. Geophys. Res. Atmos.*, *118* (13), 371–13,382; doi:10.1002/2013JD021051.

Hurwitz, M. M., I. S. Song, L. D. Oman, P. A. Newman, A. M. Molod, S. M. Frith, and J. E. Nielsen (2011b), Response of the Antarctic stratosphere to warm pool El Niño events in the GEOS CCM, *Atmos. Chem. Phys.*, *11*, 9659–9669; doi:10.5194/acp-11-9659-2011.

Hurwitz, M. M., N. Calvo, C. I. Garfinkel, A. H. Butler, S. Ineson, C. Cagnazzo, E. Manzini, and C. Peña-Ortiz (2014), Extra-tropical atmospheric response to ENSO in the CMIP5 models, *Climate Dyn.*, *43* (12), 3367–3376; doi:10.1007/s00382-014-2110-z.

Hurwitz, M. M., P. A. Newman, L. D. Oman, and A. M. Molod (2011a), Response of the Antarctic stratosphere to two types of El Niño events, *J. Atmos. Sci.*, *68*, 812–822.

Iza, M., and N. Calvo (2015), Role of stratospheric sudden warmings on the response to central Pacific El Niño, *Geophys. Res. Lett.*, *42*, 2482–2489; doi:10.1002/2014GL062935.

Jiang, N., J. D. Neelin, and M. Ghil (1995), Quasi-quadrennial and quasi-biennial variability in the equatorial Pacific, *Climate Dyn.*, *12*, 101–112.

Jin, F.-F. (1996), Tropical ocean-atmosphere interaction, the pacific cold tongue, and the El Niño Southern Oscillation, *Science*, *274*, 76–78; doi: 10.1126/science.274.5284.76.

Jin, F.-F. (1997), An equatorial recharge paradigm for ENSO, I. Conceptual model, *J. Atmos. Sci.*, *54*, 811–829.

Jin, F.-F., J. D. Neelin and M. Ghil (1994), El Niño on the devil's staircase: Annual and subharmonic steps to chaos, *Science*, *264*, 70–72; doi: 10.1126/science.264.5155.70.

Juneng, L., and F. T. Tangang (2005), Evolution of ENSO-related rainfall anomalies in Southeast Asia region and its relationship with atmosphere ocean variations in Indo-Pacific sector, *Climate Dyn.*, *25*(4), 337–350; doi:10.1007/s00382-005-0031-6.

Kalnay, E., et al. (1996), The NCEP/NCAR 40-year reanalysis project, *Bull. Amer. Meteor. Soc.*, *77*, 437–471.

Kao, H. Y., and J. -Y. Yu (2009), Contrasting eastern-Pacific and central-Pacific types of ENSO, *J. Climate*, *22*, 615–632; doi:10.1175/2008JCLI2309.1.

Karoly, D. J. (1989), Southern Hemisphere circulation features associated with El Niño–Southern Oscillation events, *J. Climate*, *2*, 1239–1252; doi:10.1175/1520-0442[1989]002, 1239:SHCFAW.2.0.CO;2.

Kerr, R. A. (2000), A North Atlantic climate pacemaker for the centuries, *Science*, *288*, 1984–1986; doi:10.1126/science.288.5473.1984.

Kessler, W. S. (2002), Is ENSO a cycle or a series of events?, *Geophys. Res. Lett.*, *29*[23], 2125; doi:10.1029/2002GL015924.

Kiladis, G. N., and H. F. Diaz (1989), Global climatic anomalies associated with extremes in the Southern Oscillation, *J. Climate*, *2*, 1069–1090.

Kim, H.-M., P. J. Webster, and J. A. Curry (2009), Impact of shifting patterns of Pacific Ocean warming on north Atlantic tropical cyclones, *Science*, *325*, 77–80.

Kim, H. -M., P. J. Webster, and J. A. Curry (2011), Modulation of North Pacific tropical cyclone activity by three phases of ENSO, *J. Climate*, *24*, 1839–1849.

Kim, J.-S., W. Zhou, X. Wang, and S. Jain (2012), El Niño Modoki and the summer precipitation variability over South Korea: A diagnostic study, *J. Meteor. Soc. Japan*, *90*, 673–684; doi: 10.2151/jmsj.2012-507.

Kim, S. -T., and J.-Y. Yu (2012), The two types of ENSO in CMIP5 models, *Geophys. Res. Lett.*, *39*, L11704; doi:10.1029/2012GL052006.

Kim, S. -T., J.-Y. Yu, A. Kumar, and H. Wang (2012), Examination of the two types of ENSO in the NCEP CFS model and its extratropical associations, *Monthly Weather Rev.*, *140*, 1908–1923; doi:10.1175/MWR-D-11-00300.1.

Kim, S.-T., W. Cai, F.-F. Jin, A. Santoso, L. Wu, E. Guilyardi, and S.-I. An (2014), Response of El Niño sea surface temperature variability to greenhouse warming, *Nature Climate Change*, *4*, 786–790; doi: 10.1038/NCLIMATE2326.

Kinter, J. L., K. Miyakoda, and S. Yang (2002), Recent change in the connection from the Asian monsoon to ENSO, *J. Climate*, *15*, 1203–1215.

Klein, S. A., B. J. Soden, and N.-C. Lau (1999), Remote sea surface temperature variations during ENSO: Evidence for a tropical atmospheric bridge, *J. Climate*, *12*, 917–932.

Knutson, T. R., S. Manabe, and D. Gu (1997), Simulated ENSO in a global coupled ocean-atmosphere model: Multidecadal amplitude modulation and CO2 sensitivity, *J. Climate*, *10*, 131–161.

Kohl, A., D. Dommenget, K. Ueyoshi, and D. Stammer (2006), The global ECCO 1952 to 2001 ocean synthesis, *ECCO Tech. Rep.*, *40*.

Kug, J.-S., F.-F. Jin, and S.-I. An (2009), Two types of El Niño events: Cold tongue El Niño and warm pool El Niño, *J. Climate*, *22*, 1499–1515; doi:10.1175/2008JCLI2624.1.

Kug, J.-S., J. Choi, S.-I. An, F.-F. Jin, and A. T. Wittenberg (2010), Warm pool and cold tongue El Niño events as simulated by the GFDL CM2.1 coupled GCM, *J. Climate*, *23*, 1226–1239; doi:10.1175/2009JCLI3293.1.

Kumar, A., and Z.-Z. Hu (2014), Interannual and interdecadal variability of ocean temperature along the equatorial Pacific in conjunction with ENSO, *Climate Dyn.*, *42* (5–6), 1243–1258; doi: 10.1007/s00382-013-1721-0.

Kumar, K. K., B. Rajagopatan, M. Hoerling, G. Bates, and M. Cane (2006), Unraveling the mystery of Indian monsoon failure during El Niño, *Science*, *314*, 115–119.

Kunz, T., K. Fraedrich, and F. Lunkeit (2009), Impact of synoptic-scale wave breaking on the NAO and its connection with the stratosphere in ERA-40*, J. Climate;* doi:10.1175/2009JCLI2750.1.

Kwok, R., and J. C. Comiso (2002), Spatial patterns of variability in Antarctic surface temperature: Connections to the South Hemisphere annular mode and the Southern Oscillation, *Geophys. Res. Lett.*, *29*, 1705; doi:10.1029/2002GL015415.

Larkin, N. K., and D. E. Harrison (2005a), On the definition of El Niño and associated seasonal average U.S. weather anomalies, *Geophys. Res. Lett*., *32*, L13705; doi:10.1029/2005GL022738.

Larkin, N. K., and D. E. Harrison (2005b), Global seasonal temperature and precipitation anomalies during El Niño autumn and winter, *Geophys. Res. Lett.*, *32*, L16705; doi:10.1029/2005GL022860.

Larson, S., S.-K. Lee, C. Wang, E.-S. Chung, and D. Enfield (2012), Impacts of non-canonical El Nino patterns on Atlantic hurricane activity, *Geophys. Res. Lett.*, *39*, L14706; doi:10.1029/2012GL052595.

Larson, S. M., and B. P. Kirtman (2014), The Pacific meridional mode as an ENSO precursor and predictor in the North American multimodel ensemble, *J. Climate*, *27*, 7018–7032; doi: http://dx.doi.org/10.1175/JCLI-D-14-00055.1.

Latif, M., and T. P. Barnett (1994), Causes of decadal climate variability over the North Pacific and North America, *Science*, *266*, 634–637.

Latif, M., D. Anderson, T. Barnett, M. Cane, R. Kleeman, A. Leetmaa, J. O'Brien, A. Rosati, and E. Schneider (1998), A review of the predictability and prediction of ENSO, *J. Geophys. Res.*, *103* (C7), 14375–14393; doi:10.1029/97JC03413.

Lau, K.-M., and P. H. Chan (1983), Short-term climate variability and atmospheric teleconnections from satellite-observed outgoing longwave radiation. Part I: Simultaneous relationships, *J. Atmos. Sci.*, *40*, 2735–2750; doi:10.1175/1520-0469[1983]040<2735:STCVAA>2.0.CO;2.

Lau, K.-M., and P. H. Chan (1985), Aspects of the 40–50 day oscillation during the northern winter as inferred from outgoing longwaveradiation, *Monthly. Weather Rev.*, *113*, 1889–1909; doi:10.1175/1520-0493[1985]113<1889:AOTDOD>2.0.CO;2.

Lau, N. C., and M. J. Nath (2004), Coupled GCM simulation of atmosphere-ocean variability associated with zonally asymmetric SST changes in the tropical Indian Ocean, *J. Climate*, *17*, 245–265.

Lee, E.-J., K.-J. Ha, and J.-G. Jhun (2014), Interdecadal changes in interannual variability of the global monsoon precipitation and interrelationships among its subcomponents, *Climate Dyn.*, *42*, 2585–2601.

Lee, S.-K., C. Wang, and D. B. Enfield (2010), On the impact of central Pacific warming events on Atlantic tropical storm activity, *Geophys. Res. Lett.*, *37*, L17702; doi:10.1029/2010GL044459.

Lee, T., and coauthors (2010), Record warming in the South Pacific and western Antarctica associated with the strong central Pacific El Niño in 2009–10, *Geophys. Res. Lett.*, *37*, L19704; doi:10.1029/2010GL044865.

Lee, T., and M. J. McPhaden (2010), Increasing intensity of El Niño in the central-equatorial Pacific, *Geophys. Res. Lett.*, *37*, L14603; doi:10.1029/2010GL044007.

L'Heureux, M. L., and D. W. J. Thompson (2006), Observed relationships between the El Niño–Southern Oscillation and the extratropical zonal-mean circulation, *J. Climate*, *19*, 276–287; doi:10.1175/JCLI3617.1.

L'Heureux, M. L., S. Lee, and B. Lyon (2013), Recent multidecadal strengthening of the Walker circulation across the tropical Pacific, *Nature Climate Change*, *3*, 571–576.

Li, Y., and S. Yang (2010), A dynamical index for the east Asian winter monsoon, *J. Climate*, *23*, 4255–4262.

Liang, Y.-C., J.-Y. Yu, M.-H. Lo, and C. Wang (2015), The changing influence of El Niño on the Great Plains low-level jet, *Atmosph. Sci. Lett.*; doi: 10.1002/asl.590.

Liang, Y.-C., M.-H. Lo, and J.-Y. Yu (2014), Asymmetric responses of land hydroclimatology to two types of El Niño in the Mississippi River basin, *Geophys. Res. Lett.*, *41*, 582–588; doi:10.1002/2013GL058828.

Lim, E.-P., and H. H. Hendon, D. Hudson, G. Wang, and O. Alves (2009), Dynamical forecast of inter–El Niño variations of tropical SST and Australian spring rainfall, *Monthly Weather Rev.*, *137*, 3796–3810; doi:10.1175/2009MWR2904.1.

Lin, C.-Y., J.-Y. Yu, and H. H. Hsu (2014), CMIP5 model simulations of the Pacific meridional mode and its connection to the two types of ENSO, *Int. J. Climatol.*; doi:10.1002/joc.4130.

Lin, P., Q. Fu, D. L. Hartmann (2012), Impact of tropical SST on stratospheric planetary waves in the Southern Hemisphere, *J. Climate*, *25*, 5030–5046; doi:10.1175/JCLI-D-11-00378.1.

Linkin, M. E., and S. Nigam (2008), The north Pacific Oscillation-west Pacific teleconnection pattern: Mature-phase structure and winter impacts, *J. Climate*, *21*, 1979–1997; doi:10.1175/2007JCLI2048.1.

Liu, J., J. A. Curry, and D. G. Martinson (2004), Interpretation of recent Antarctic sea ice variability, *Geophys. Res. Lett.*, *31*, L02205; doi:10.1029/2003GL018732.

Liu, Q.-Y., D. Wang, X. Wang, Y. Shu, Q. Xie, J. Chen (2014), Thermal variations in the South China Sea associated with the eastern and central Pacific El Niño events and their mechanisms, *J. Geophys. Res. Oceans*, *119*, 8955–8972; doi:10.1002/2014JC010429.

Liu, Z., and M. Alexander (2007), Atmospheric bridge, oceanic tunnel, and global climatic teleconnections, *Rev. Geophys.*, *45*, RG2005; doi:10.1029/2005RG00017.

Livezey, R. E., M. Masutani, A. Leetmaa, A., H. Rui, M. Ji, and A. Kumar (1997), Teleconnective response of the Pacific–North American region atmosphere to large central equatorial Pacific SST anomalies, *J. Climate*, *10*, 1787–1820.

Lu, J., G. Chen, and D. M. W. Frierson (2008), Response of the zonal mean atmospheric circulation to El Niño versus global warming, *J. Climate*, *21*, 5835–5851.

Luo, J. J., S. Masson, S. Behera, S. Shingu, and T. Yamagata (2005), Seasonal climate predictability in a coupled OAGCM using a different approach for ensemble forecasts, *J. Climate*, *18*, 4474–4497.

Maloney, E. D., and coauthors (2014), North American climate in CMIP5 experiments: Part III: Assessment of twenty-first-century projections, *J. Climate*, *27*, 2230–2270; doi: http://dx.doi.org/10.1175/JCLI-D-13-00273.1.

Mantua, N. J., and D. S. Battisti (1995), Aperiodic variability in the Zebiak-cane coupled ocean-atmosphere model: Air-sea interactions in the western equatorial Pacific, *J. Climate*, *8*, 2897–2927; doi: http://dx.doi.org/10.1175/1520-0442[1995]008<2897:AVITZC>2.0.CO;2.

Mantua, N. J., S. R. Hare, Y. Zhang, J. M. Wallace, and R. C. Francis (1997), A Pacific interdecadal climate oscillation with impacts on salmon production, *Bull. Amer. Meteor. Soc.*, *78*, 1069–1079.

Manzini, E., M. A. Giorgetta, M. Esch, L. Kornblueh, and E. Roeckner (2006), The influence of sea surface temperatures on the northern winter stratosphere: Ensemble simulations with the MAECHAM5 model, *J. Climate*, *19*, 3863–3881; doi:10.1175/JCLI3826.1.

McBride, J., M. Haylock, and N. Nicholls (2003), Relationships between the maritime continent heat source and the El Niño–Southern Oscillation phenomenon, *J. Climate*, *16* (17), 2905–2914; doi:10.1175/1520–0442 [2003]016<2905:RBTMCH>2.0.CO;2.

McCreary, J. P., and P. Lu (1994), Interaction between the subtropical and equatorial ocean circulations: The subtropical cell, *J. Phys. Oceanogr.*, *24*, 466–497.

McIntyre, M. E. (1982), How well do we understand the dynamics of stratospheric warming?, *J. Meteor. Soc. Japan*, *60*, 37–64.

McPhaden, M. J. (2008), Evolution of the 2006–2007 El Niño: The role of intraseasonal to interannual time scale dynamics, *Adv. Geosci.*, *14*, 219–230; doi:10.5194/adgeo-14-219-2008.

McPhaden, M. J. (2012), A 21st century shift in the relationship between ENSO SST and warm water volume anomalies, *Geophys. Res. Lett.*, *39*, L09706; doi:10.1029/2012GL051826.

McPhaden, M. J., and D. Zhang (2002), Slowdown of the meridional overturning circulation in the upper Pacific Ocean, *Nature*, *415*, 603–608.

McPhaden, M. J., T. Lee, and D. McClurg (2011), El Niño and its relationship to changing background conditions in the tropical Pacific Ocean, *Geophys. Res. Lett.*, *38*, L15709; doi:10.1029/2011GL048275.

Mechoso, C. R., D. L. Hartmann, and J. D. Farrara (1985), Climatology and interannual variability of wave, mean-flow interaction in the Southern Hemisphere, *J. Atmos. Sci.*, *42*, 2189–2206.

Meehl, G. A., and H. Teng (2007), Multi-model changes in El Niño teleconnections over North America in a future warmer climate, *Climate Dyn.*, *29*, 779–790; doi:10.1007/s00382-007-0268-3.

Meehl, G. A., and W. M. Washington (1996), El Niño-like climate change in a model with increased atmospheric CO2 concentrations, *Nature*, *382* (6586), 56–60.

Meehl, G. A., et al. (2007), The WCRP CMIP3 multimodel dataset: A new era in climate change research, *Bull. Amer. Meteorol. Soc.*, *88*, 1383–1394; doi:10.1175/BAMS-88-9-1383.

Meehl, G. A., G. W. Branstator, and W. M. Washington (1993), Tropical Pacific interannual variability and CO2 climate change, *J. Climate*, *6*, 42–63.

Meehl, G. A., W. D. Collins, B. A. Boville, J. T. Kiehl, T. M. L.Wigley, and J. M. Arblaster (2000), Response of the NCAR climate system model to increased CO2 and the role of physical processes, *J. Climate*, *13* (11), 1879–1898.

Meinen, C. S., and M. J. McPhaden (2000), Observations of warm water volume changes in the equatorial Pacific and their relationship to El Niño and La Niña, *J. Climate*, *13*, 3551–3559; doi:10.1175/1520-0442[2000] 013<3551:OOWWVC>2.0.CO;2.

Merrifield, M. A. (2011), A shift in western tropical Pacific sea level trends during the 1990s, *J. Climate*, *24*, 4126–4138; doi: http://dx.doi.org/10.1175/2011JCLI3932.1.

Merryfield, W. J. (2006), Changes to ENSO under CO2 doubling in a multimodel ensemble, *J. Climate*, *19*, 4009–4027.

Minobe, S. (2000), Spatio-temporal structure of the pentadecadal variability over the North Pacific, *Prog. Oceanogr.*, *47*, 381–408; doi:10.1016/S0079-6611[00]00042-2.

Minobe, S. (2002), Interannual to interdecadal changes in the Bering Sea and concurrent 1998/99 changes over the North Pacific, *Prog. Oceanogr.*, *55*, 45–64; doi:10.1016/S0079-6611[02]00069-1.

Mo, K. C. (2000), Relationships between interdecadal variability in the Southern Hemisphere and sea surface temperature anomalies, *J. Climate*, *13*, 3599–3610.

Mo, K. C. (2010), Interdecadal modulation of the impact of ENSO on precipitation and temperature over the United States, *J. Climate*, *23*, 3639–3656; doi:10.1175/2010JCLI3553.1.

Mo, K. C., and M. Ghil (1987), Statistics and dynamics of persistent anomalies, *J. Atmos. Sci.*, *44*, 877–902; doi:10.1175/1520-0469[1987]044,0877:SADOPA.2.0.CO;2.

Mo, K. C., and R. E. Livezey (1986), Tropical-extratropical geopotential height teleconnections during the Northern Hemisphere winter, *Monthly Weather Rev.*, *114*, 2488–2515.

Mo, K. C., and R. W. Higgins (1998), Tropical convection and precipitation regimes in the western United States, *J. Climate*, *11*, 2404–2423.

Monahan, A. H. (2001), Nonlinear principal component analysis: Tropical Indo-Pacific sea surface temperature and sea level pressure, *J. Climate*, *14*, 219–233.

Na, H., B.-G. Jang, W.-M. Choi, and K.-Y. Kim (2011), Statistical simulations of the future 50-year statistics of cold-tongue

El Niño and warm-pool El Niño, *Asia-Pacific J. Atmos. Sci.*, *47*, 223–233; doi:10.1007/s13143-011-0011-1.

Neale, R. B., J. Richter, S. Park, P. H. Lauritzen, S. J. Vavrus, P. J. Rasch, and M. Zhang (2013), The mean climate of the community atmosphere model (CAM4) in forced SST and fully coupled experiments, *J. Climate*, *26*, 5150–5168; doi:10.1175/JCLI-D-12-00236.1.

Neelin, J. D. (1991), The slow sea surface temperature mode and the fast-wave limit: Analytic theory for tropical interannual oscillations and experiments in a hybrid coupled model, *J. Atmos. Sci.*, *48*, 584–606.

Neelin, J. D., and F.-F. Jin (1993), Modes of interannual tropical ocean-atmosphere interaction-a unified view, II, Analytical results in the weak coupling limit, *J. Atmos. Sci.*, *50*, 3504–3522.

Neelin, J. D., D. S. Battisti, A. C. Hirst, F.-F. Jin, Y. Wakata, T. Yamagata, and S. E. Zebiak (1998), ENSO theory, *J. Geophys. Res.*, *103* (C7), 14261–14290; doi:10.1029/97JC03424.

Newman, M., et al. (2015), The Pacific decadal oscillation, revisited, *Bull. Amer. Meteor. Soc.* (submitted).

Newman, M., S.-I. Shin, and M. A. Alexander (2011), Natural variation in ENSO flavors. *Geophys. Res. Lett.,* L14705; doi:10.1029/2011GL047658.

Nishii, K., H. Nakamura, and Y. J. Orsolini (2010), Cooling of the wintertime Arctic stratosphere induced by the western Pacific teleconnection pattern, *Geophys. Res. Lett.*, *371*, L13805; doi:10.1029/2010GL043551.

Noda, A., K. Yoshimatsu, S. Yukimoto, K. Yamahuchi, and S. Yamaki (1999), Relationship between natural variability and CO2-induced warming pattern: MRI AOGCM experiment, in *10th Symposium on Global Change Studies*, American Meteorological Society Publication.

Paek, H., J.-Y., Yu, J.-W. Hwu, M.-M. Lu, and T. Gao (2015), A source of AGCM bias in simulating the western Pacific subtropical high: Different sensitivities to the two types of ENSO, *Monthly Weather Rev.*, *143*, 2348–2362.

Peterson, W. T., and F. B. Schwing (2003), A new climate regime in northeast pacific ecosystems, *Geophys. Res. Lett.*, *30*, 1896; doi:10.1029/2003GL017528.

Philander, S. G. (1999), A review of tropical ocean–atmosphere interactions, *Tellus A*, *51* (1), 71–90.

Pierce, D. W., T. P. Barnett, and M. Latif (2000), Connections between the Pacific Ocean tropics and midlatitudes on decadal timescales, *J. Climate*, *13*, 1173–1194.

Qian, C., J. -Y. Yu, and G. Chen (2014), Decadal summer drought frequency in China: The increasing influence of the Atlantic multi-decadal oscillation, *Environ. Res. Lett.*, *9* (12), 124004; doi:10.1088/1748-9326/9/12/124004.

Qiu, B., and S. Chen (2012), Multidecadal sea level and gyre circulation variability in the northwestern tropical Pacific Ocean, *J. Phys. Oceanogr*., *42*, 193–206; doi: http://dx.doi.org/10.1175/JPO-D-11-061.1.

Rajagopolan, B., U. Lall, and M. Cane (1997), Anomalous ENSO occurrences: An alternate view, *J. Climate*, *10*, 2351–2357.

Rasmusson, E. M., and T. H. Carpenter (1982), Variations in tropical sea surface temperature and surface wind fields associated with the Southern Oscillation/El Niño, *Monthly Weather Rev*., *110*, 354–384; doi: http://dx.doi.org/10.1175/1520-0493[1982]110<0354:VITSST>2.0.CO;2.

Rasmusson, E. M., X. Wang, and C. F. Ropelewski (1990), The biennial component of ENSO variability, *J. Mar. Syst.*, *1*, 71–90; doi:10.1016/0924-7963[90]90153-2.

Ratnam, J. V., S. K. Behera, Y. Masumoto, and T. Yamagata (2014), Remote effects of El Niño on Modoki events on the austral summer precipitation of southern Africa, *J. Climate*, *27*, 3802–3815; doi:10.1175/JCLI-D-13-00431.1.

Rayner, N. A., et al. (2003), Global analyses of sea surface temperature, sea ice, and night marine air temperature since the late nineteenth century, *J. Geophys. Res.*, *108* (D14), 4407.

Ren, H.-L., and F.-F. Jin (2011), Niño indices for two types of ENSO, *Geophys. Res. Lett.*, *38*, L04704; doi: 10.1029/2010GL046031.

Ren, H.-L., and F.-F. Jin (2013), Recharge oscillator mechanisms in two types of ENSO, *J. Climate*, *26*, 6506–6523. doi:10.1175/JCLI-D-12-00601.1.

Rodgers, K. B., P. Friederichs, and M. Latif (2004), Tropical Pacific decadal variability and its relation to decadal modulations of ENSO, *J. Climate*, *17*, 3761–3774.

Rodrigues, R. R., R. J. Haarsma, E. J. D. Campos, T. Ambrizzi (2011), The impacts of inter-El Niño variability on the tropical Atlantic and northeast Brazil climate, *J. Climate*, *24*, 3402–3422.

Rogers, J. C. (1981), The North Pacific Oscillation, *Int. J. Climatol.*, *1*, 39–57; doi:10.1002/joc.3370010106.

Ropelewski, C. F., and M. S. Halpert (1986), North American precipitation and temperature patterns associated with the El Niño/Southern Oscillation, *Monthly Weather Rev.*, *114*, 2352–2362.

Ropelewski, C. F., and M. S. Halpert (1987), Global and regional scale precipitation patterns associated with the El Nino Southern Oscillation, *Monthly Weather Rev.*, *115*, 1606–1626.

Ropelewski, C. F., and M. S. Halpert (1989), Precipitation patterns associated with the high index phase of the Southern Oscillation, *J. Climate*, *2*, 268–284.

Saji, N. H., B. N. Goswami, P. N. Vinayachandran, and T. Yamagata (1999), A dipole mode in the tropical Indian Ocean, *Nature*, *401*, 360–363.

Sassi, F., D. Kinnison, B. A. Boville, R. R. Garcia, and R. Roble (2004), Effect of El Niño–Southern Oscillation on the dynamical, thermal, and chemical structure of the middle atmosphere, *J. Geophys. Res.*, *109*, D17108; doi:10.1029/2003JD004434.

Schlesinger, M. E., and N. Ramankutty (1994), An oscillation in the global climate system of period 65–70 years, *Nature*, *367*, 723–726; doi:10.1038/367723a0.

Schneider, D. P., Y. Okumura, and C. Deser (2012), Observed Antarctic interannual climate variability and tropical linkages, *J. Climate*, *25*, 4048–4066; doi:10.1175/JCLI-D-11-00273.1.

Schopf, P. S., and R. J. Burgman (2006), A simple mechanism for ENSO residuals and asymmetry, *J. Climate*, *19*, 3167–3179.

Schott. F. A., S. P. Xie, and J. McCreary (2009), Indian Ocean circulation and climate variability, *Rev. Geophys.*, *47*, RG1002; doi:10.1029/2007RG000245.

Seager, R., N. Harnik, Y. Kushnir, W. Robinson, and J. Miller (2003), Mechanisms of hemispherically symmetric climate variability, *J. Climate*, *16*, 2960–2978.

Sheffield, J., and coauthors (2013a), North American climate in CMIP5 experiments, Part I: Evaluation of historical simulations of continental and regional climatology, *J. Climate*, *26*, 9209–9245; doi: http://dx.doi.org/10.1175/JCLI-D-12-00592.1.

Sheffield, J., and coauthors (2013b), North American climate in CMIP5 experiments, Part II: Evaluation of 20th century intraseasonal to decadal variability, *J. Climate*, *23*, 9247–9290.

Sheffield, J., and coauthors (2014), Regional climate processes and projections for North America: CMIP3/CMIP5 differences, attribution and outstanding issues, *NOAA Tech. Rep., OAR CPO-2*.

Smith, T. M., R. W. Reynolds, T. C. Peterson, and J. Lawrimore (2008), Improvements to NOAA's historical merged land-ocean surface temperature analysis (1880–2006), *J. Climate*, *21*, 2283–2296.

Son, S. -W., A. Purich, H. H. Hendon, B. M. Kim, and L. M. Polvani (2013), Improved seasonal forecast using ozone hole variability? *Geophys. Res. Lett.*, *40*, 6231–6235; doi:10.1002/2013GL057731.

Song, H.-J., E. Choi, G.-H. Lim, Y. H. Kim, J.-S. Kug, and S.-W. Yeh (2011), The central Pacific as the export region of the El Niño–Southern Oscillation sea surface temperature anomaly to Antarctic sea ice, *J. Geophys. Res.*, *116*, D21113; doi:10.1029/2011JD015645.

Stammerjohn, S. E., D. G. Martinson, R. C. Smith, X. Yuan, and D. Rind (2008), Trends in Antarctic annual sea ice retreat and advance and their relation to El Niño–Southern Oscillation and southern annular mode variability, *J. Geophys. Res.*, *113*, C03S90; doi:10.1029/2007JC004269.

Stevenson, S., B. Fox-Kemper, M. Jochum, R. Neale, C. Deser, and G. Meehl (2012), Will there be a significant change to El Niño in the twenty-first century?, *J. Climate*, *25*, 2129–2145; doi:10.1175/JCLI-D-11-00252.1.

Su, J., R. Zhang, T. Li, X. Rong, J.-S. Kug, and C.-C. Hong (2010), Causes of the El Niño and La Niña amplitude asymmetry in the equatorial eastern Pacific, *J. Climate*, *23*, 605–617.

Suarez, M. J., and P. S. Schopf (1988), A delayed action oscillator for ENSO, *J. Atmos. Sci.*, *45*, 3283–3287; doi:10.1175/1520-0469%281988%29045<3283%3AADAOFE>2.0.CO%3B2.

Sui, C. H., P. H. Chung, and T. Li (2007), Interannual and interdecadal variability of the summertime western North Pacific subtropical high, *Geophys. Res. Lett.*, *34*, L11701; doi:10.1029/2006GL029204.

Sun, D.-Z., and T. Zhang (2006), A regulatory effect of ENSO on the timemean thermal stratification of the equatorial upper ocean, *Geophys. Res. Lett.*, *33*, L07710; doi:10.1029/2005GL025296.

Sun, F., and J. -Y. Yu (2009), A 10–15-yr modulation cycle of ENSO intensity, *J. Climate*, *22*, 1718–1735; doi: http://dx.doi.org/10.1175/2008JCLI2285.1.

Sung, M.-K., B.-M. Kim, and S.-I. An (2014), Altered atmospheric responses to eastern Pacific and central Pacific El Niños over the North Atlantic region due to stratospheric interference, *Climate Dyn.*, *42*, 159–170; doi:10.1007/s00382-012-1661-0.

Takahashi, K., A. Montecinos, K. Goubanova, and B. Dewitte (2011), ENSO regimes: Reinterpreting the canonical and Modoki El Niño, *Geophys. Res. Lett.*, *38*, L10704; doi: 10.1029/2011GL047364.

Tang, B. H., and J. D. Neelin (2004), ENSO influence on Atlantic hurricanes via tropospheric warming, *Geophys. Res. Lett.*, *31*, L24204; doi:10.1029/2004GL021072.

Taschetto, A. S., and M. H. England (2009), El Niño Modoki impacts on Australian rainfall, *J. Climate*, *22*, 3167–3174.

Taschetto, A. S., A. Sen Gupta, N. C. Jourdain, A. Santoso, C. C. Ummenhofer, and M. H. England (2014), Cold tongue and warm pool ENSO events in CMIP5: Mean state and future projections, *J. Climate*, *27*, 2861–2885; doi:10.1175/JCLI-D-13-00437.1.

Taylor, K. E., R. J. Stouffer, and G. A. Meehl (2012), An overview of CMIP5 and the experiment design, *Bull. Amer. Meteor. Soc.*, *93*, 485–498.

Tett, S. (1995), Simulation of El Niño–Southern Oscillation-like variability in a global AOGCM and its response to CO2 increase, *J. Climate*, *8* (6), 1473–1502.

Thompson, D. W. J., and J. M. Wallace (1998), The Arctic Oscillation signature in the wintertime geopotential height and temperature fields, *Geophys. Res. Lett.*, *25*, 1297–1300; doi:10.1029/98GL00950.

Thompson, D. W. J., and J. M. Wallace (2000), Annular modes in the extratropical circulation, Part I: Month-to-month variability, *J. Climate*, *13*, 1000–1016.

Timmermann, A. (2003), Decadal ENSO amplitude modulations: A nonlinear mechanism, *Global Planet. Change*, *37*, 135–156.

Timmermann, A., and F.-F. Jin (2002), A nonlinear mechanism for decadal El Niño amplitude changes, *Geophys. Res. Lett.*, *29*, 1003; doi:10.1029/2001GL013369.

Timmermann, A., J. Oberhuber, A. Bacher, M. Esch, M. Latif, and E. Roeckner (1999), Increased El Niño frequency in a climate model forced by future greenhouse warming, *Nature*, *398*, 694–697.

Tokinaga, H., S.-P. Xie, C. Deser, Y. Kosaka, and Y. M. Okumura (2012), Slowdown of the Walker circulation driven by tropical Indo-Pacific warming, *Nature*, *491*, 439–443; doi:10.1038/nature11576.

Torrence, C., and P. J. Webster (1999), Interdecadal changes in the ENSO-monsoon system, *J. Climate*, *12*, 2679–2690.

Trenberth, K. E., and D. P. Stepaniak (2001), Indices of El Niño evolution, *J. Climate*, *14*, 1697–1701. doi: http://dx.doi.org/10.1175/1520-0442[2001]014<1697:LIOENO>2.0.CO;2.

Trenberth, K. E., and T. J. Hoar (1996), The 1990–1995 E1 Niño–Southern Oscillation event: Longest on record, *Geophys. Res. Lett.*, *23*, 57–60.

Tu, J., C. Chou, and P. Chu (2009), The abrupt shift of typhoon activity in the vicinity of Taiwan and its association with western North Pacific–East Asian climate change, *J. Climate*, *22*, 3617–3628.

Tziperman, E., L. Stone, M. Cane, and H. Jarosh (1994), El Niño chaos: Overlapping of resonances between the seasonal cycle and the Pacific Ocean-atmosphere oscillator, *Science*, *264*, 72.

Tziperman, E., M. Cane, and S. E. Zebiak (1995), Irregularity and locking to the seasonal cycle in an ENSO prediction

model as explained by the quasi-periodicity route to chaos, *J. Atmos. Sci.*, *52*, 293–306.

van Oldenborgh, G. J., S. Y. Philip, and M. Collins (2005), El Niño in a changing climate: A multi-model study, *Ocean Sci.*, *1*, 81–95; doi:10.5194/os-1-81-2005.

Vecchi, G. A., and B. J. Soden (2007), Global warming and the weakening of the tropical circulation, *J. Climate*, *20*, 4316–40.

Vecchi, G. A., et al. (2006), Weakening of tropical Pacific atmospheric circulation due to anthropogenic forcing, *Nature*, *441*, 73–76.

Venzke, S., M. Latif, and A. Villwock (2000), The coupled GCM ECHO-2, Part II: Indian Ocean response to ENSO, *J. Climate*, *13*, 1317–1383.

Verdon, D. C., and S. W. Franks (2006), Long-term behaviour of ENSO: Interactions with the PDO over the past 400 years inferred from paleoclimate records, *Geophys. Res. Lett.*, *33*, L06712; doi:10.1029/2005GL025052.

Vimont, D. J., D. S. Battisti, and A. C. Hirst (2001), Footprinting: A seasonal connection between the tropics and mid-latitudes, *Geophys. Res. Lett.*, *28*, 3923–3926; doi:10.1029/2001GL013435.

Vimont, D. J., J. M. Wallace, and D. S. Battisti (2003), The seasonal footprinting mechanism in the Pacific: Implications for ENSO, *J. Climate*, *16*, 2668–2675; doi:10.1175/1520-0442%282003%29016<2668%3ATSFMIT>2.0.CO%3B2.

Vimont, D. J., M. Alexander, and A. Fontaine (2009), Midlatitude excitation of tropical variability in the Pacific: The role of thermodynamic coupling and seasonality, *J. Climate*, *22* (3), 518–534; doi:10.1175/2008JCLI2220.1.

Walker, G. T., and E. W. Bliss (1932), World weather V Mem, *R. Meteor. Soc.*, *4*, 53–84.

Wallace, J. M., and D. S. Gutzler (1981), Teleconnections in the potential height field during the Northern Hemisphere winter, *Monthly Weather Rev.*, *109*, 784–812.

Wang, B., and S. -I. An (2001), Why the properties of El Niño change in the late 1970s?, *Geophys. Res. Lett.*, *28*, 3709–3712.

Wang, B., and Y. Wang (1996), Temporal structure of the Southern Oscillation as revealed by a waveform and a wavelet transform, *J. Climate*, *9*, 1586–1598. doi: http://dx.doi.org/10.1175/1520-0442[1996]009<1586:TSOTSO>2.0.CO;2.

Wang, B., B. Xiang, and J.-Y. Lee (2013), Subtropical high predictability establishes a promising way for monsoon and tropical storm predictions, *PNAS*, *110*, 2718–2722.

Wang, B., R. Wu, and X. Fu (2000), Pacific–East Asian teleconnection: How does ENSO affect East Asian climate?, *J. Climate*, *13*, 1517–1536.

Wang, C., and R. H. Weisberg (1998), Climate variability of the coupled tropical-extratropical ocean-atmosphere system, *Geophys. Res. Lett.*, *25*, 3979–3982.

Wang, C., and X. Wang (2013), Classifying El Niño Modoki I and II by different impacts on rainfall in southern China and typhoon tracks, *J. Climate*, *26*, 1322–1338; doi: 10.1175/JCLI-D-12-00107.1.

Wang, C., C. Deser, J.-Y. Yu, P. DiNezio, and A. Clement (2015), El Nino and Southern Oscillation (ENSO): A review, A chapter for Springer book: *Coral Reefs of the Eastern Pacific*, in press.

Wang, C., R. H. Weisberg, and J. I. Virmani (1999), Western Pacific interannual variability associated with the El Niño–Southern Oscillation, *J. Geophys. Res.*, *104*, 5131–5149. DOI: 10.1029/1998JC900090.

Wang, D., Q. Liu, R. X. Huang, Y. Du, and T. Qu (2006), Interannual variability of the South China Sea throughflow inferred from wind data and an ocean data assimilation product, *Geophys. Res. Lett.*, *33*, L14605; doi:10.1029/2006GL026316.

Wang, G., and H. H. Hendon (2007), Sensitivity of Australian rainfall to inter–El Niño variations, *J. Climate*, *20*, 4211–4226.

Wang, H., and R. Fu (2000), Influences of ENSO SST anomalies and winter storm tracks on the interannual variability of upper-troposphere water vapor over the Northern Hemisphere extratropics, *J. Climate*, *13*, 59–73.

Wang, S.-Y., M. L'Heureux, and H. -H. Chia (2012), ENSO prediction one year in advance using western North Pacific sea surface temperatures, *Geophys. Res. Lett.*, *39*, L05702; doi:10.1029/2012GL050909.

Wang, S.-Y., M. L'Heureux, and J. H. Yoon (2013), Are greenhouse gases changing ENSO precursors in the western North Pacific?, *J. Climate*, *26* (17), 6309–6322.

Wang, X., and C. Wang (2014), Different impacts of various El Niño events on the Indian Ocean dipole, *Climate Dyn.*, *42*, 991–1005; doi: 10.1007/s00382-013-1711-2.

Wang, X., W. Zhou, C. Li, and D. Wang (2014), Comparison of the impact of two types of El Niño on tropical cyclone genesis over the South China Sea, *Int. J. Climatol.*, *34*, 2651–2660; doi: 10.1002/joc.3865.

Weare, B. C., A. R. Navato, and R. E. Newell (1976), Empirical orthogonal analysis of Pacific sea surface temperatures, *J. Phys. Ocean*, *6*, 671–678.

Webster, P. J., A. M. Moore, J. P. Loschnigg, and R. R. Leben (1999), Coupled ocean-atmosphere dynamics in the Indian Ocean during 1997–98, *Nature*, *401*, 356–360.

Weisberg, R. H., and C. Wang (1997), A western Pacific oscillator paradigm for the El Niño–Southern Oscillation, *Geophy. Res. Lett.*, *24*, 779–782; doi: 10.1029/97GL00689.

Weng, H., K. Ashok, S. K. Behera, S. A. Rao, and T. Yamagada (2007), Impacts of recent El Nino Modoki on droughts/floods in the Pacific rim during boreal summer, *Climate Dyn.*, *29*, 113–129; doi:10.1007/s00382-007-0234-0.

Weng, H., S. K. Behera, and T. Yamagada (2009), Anomalous winter climate conditions in the Pacific rim during recent El Nino Modoki and El Nino events, *Climate Dyn.*, *32*, 663–674; doi:10.1007/s00382-008-0394-6.

Wittenberg, A. T. (2009), Are historical records sufficient to constrain ENSO simulations?, *Geophys. Res. Lett.*, *36*, L12702; doi:10.1029/2009GL038710.

Wyrtki, K. (1975), El Niño: The dynamic response of the equatorial Pacific Ocean to atmospheric forcing, *J. Phys. Oceanogr.*, *5*, 572–584; doi:10.1175/1520-0485%281975%29005<0572%3AENTDRO>2.0.CO%3B2.

Xiang, B., B. Wang, and T. Li (2013), A new paradigm for the predominance of standing Central Pacific warming after the late 1990s, *Climate Dyn.*, *41* (2), 327–340; doi: 10.1007/s00382-012-1427-8.

Xie, F., J. Li, W. Tian, J. Feng, and Y. Huo (2012), Signals of El Niño Modoki in the tropical tropopause

layer and stratosphere, *Atmos. Chem. Phys.*, *12*, 5259–5273; doi:10.5194/acp-12-5259-2012.

Xie, S.-P., and S. G. H. Philander (1994), A coupled ocean-atmosphere model of relevance to the ITCZ in the eastern Pacific, *Tellus*, *46A*, 340–350; doi:10.1034/j.1600-0870.1994.t01-1-00001.x.

Xie, S.-P., C. Deser, G. A. Vecchi, J. Ma, H. Teng, and A. T. Wittenberg (2010), Global warming pattern formation: Sea surface temperature and rainfall, *J. Climate*, *23*, 966–986; doi:10.1175/2009JCLI3329.1.

Xie, S.-P., H. Annamalai, F. Schott, and J. P. McCreary Jr. (2002), Origin and predictability of South Indian Ocean climate variability, *J. Climate*, *15* (8), 864–874.

Xie, S. -P., K. Hu, J. Hafner, H. Tokinaga, Y. Du, G. Huang, and T. Sampe (2009), Indian Ocean capacitor effect on Indo–Western Pacific climate during the summer following El Niño, *J. Climate*, *22* (3).

Xie, S.-P., Q. Xie, D. Wang, and W. T. Liu (2003), Summer upwelling in the South China Sea and its role in regional climate variations, *J. Geophys. Res.*, *108* (C8), 3261; doi:10.1029/2003JC001867.

Xu, B., J. Cao, J. Hansen, T. Yao, D. Joswia, N. Wang, G. Wu, M. Wang, H. Zhao, W. Yang, X. Liu, and J. He (2009), Black soot and the survival of Tibetan glaciers, *Proc. Nat. Acad. Sci.*, *106*, 22114.

Xu, Z., K. Fan, and H. Wang (2015), Decadal variation of summer precipitation over China and associated atmospheric circulation after the late 1990s, *J. Climate*, *28* (10), 4086–4106.

Xue, Y., M. Chen, A. Kumar, Z.-Z. Hu, and W. Wang (2013), Prediction skill and bias of tropical Pacific sea surface temperatures in the NCEP climate forecast system version 2, *J. Climate*, *26*, 5358–5378; doi:10.1175/JCLI-D-12-00600.1.

Yadav, R. K., D. A. Ramu, and A. P. Dimri (2013), On the relationship between ENSO patterns and winter precipitation over north and central India, *Global Planet. Change*, *107*, 50–58; doi:10.1016/j.gloplacha.2013.04.006.

Yang, J., Q. Liu, S.-P. Xie, Z. Liu, and L. Wu (2007), Impact of the Indian Ocean SST basin mode on the Asian summer monsoon, *Geophys. Res. Lett.*, *34*, L02708; doi:10.1029/2006GL028571.

Yang, S., and X. Jiang (2014), Prediction of eastern and central Pacific ENSO events and their impacts on East Asian climate by the NCEP climate forecast system, *J. Climate*, *27*, 4451–4472.

Yeh, S.-W., and B. P. Kirtman (2004), Tropical Pacific decadal variability and ENSO amplitude modulation in a CGCM, *J. Geophys. Res.*, *109*, C11009; doi:10.1029/2004JC002442.

Yeh, S. -W., and B. P. Kirtman (2007), ENSO amplitude changes due to climate change projections in different coupled models, *J. Climate*, *20*, 203–217.

Yeh, S.-W., B. P. Kirtman, J.-S. Kug, W. Park, and M. Latif (2011), Natural variability of the central Pacific El Niño event on multi-centennial timescales, *Geophys. Res. Lett.*, *38*, L02704; doi:10.1029/2010GL045886.

Yeh, S. W., J. S. Kug, B. Dewitte, M. H. Kwon, B. P. Kirtman, and F.-F. Jin (2009), El Niño in a changing climate, *Nature*, *461*, 511–514; doi:10.1038/nature08316.

Yeh, S.-W., X. Wang, C. Wang, and B. Dewitte (2015), On the relationship between the North Pacific climate variability and the central Pacific El Niño, *J. Climate*, *28*, 663–677; doi: http://dx.doi.org/10.1175/JCLI-D-14-00137.1.

Yeo, S. -R., and K. -Y. Kim (2015), Decadal changes in the Southern Hemisphere sea surface temperature in association with El Niño–Southern Oscillation and southern annular mode, *Climate Dyn.*, 1–16, http://dx.doi.org/10.1007/s00382-015-2535-z.

Yeo, S. -R., K. Y. Kim, S. W. Yeh, B. M. Kim, T. Shim, and J. G. Jhun (2014), Recent climate variation in the Bering and Chukchi seas and its linkages to large-scale circulation in the Pacific, *Climate Dyn.*, *42* (9–10), 2423–2437.

Yu, J.-Y., and H.-Y. Kao (2007), Decadal changes of ENSO persistence barrier in SST and ocean heat content indices: 1958–2001, *J. Geophys. Res.*, *112*, D13106; doi:10.1029/2006JD007654.

Yu, J.-Y., and K. M. Lau (2004), Contrasting Indian Ocean SST variability with and without ENSO influence: A coupled atmosphere-ocean GCM study, *Meteor. Atmos. Phys.*, *90*, 179–191; doi:10.1007/s00703-004-0094-7.

Yu, J.-Y., and S. T. Kim (2010a), Identification of central-Pacific and eastern-Pacific types of ENSO in CMIP3 models, *Geophys. Res. Lett.*, *37*, L15705; doi:10.1029/2010GL044082.

Yu, J.-Y., and S. T. Kim (2010b), Three evolution patterns of central-Pacific El Niño, *Geophys. Res. Lett.*, *37*, L08706; doi:10.1029/2010GL042810.

Yu, J.-Y., and S. T. Kim (2011a), Relationships between extratropical sea level pressure variations and the central-Pacific and eastern-Pacific types of ENSO, *J. Climate*, *24*, 708–720; doi:10.1175/2010JCLI3688.1.

Yu, J.-Y., and S.-T. Kim (2011b), Reversed spatial asymmetries between El Niño and La Niña and their linkage to decadal ENSO modulation in CMIP3 models, *J. Climate*, *24*, 5423–5434.

Yu, J.-Y., and Y. Zou (2013), The enhanced drying effect of Central-Pacific El Niño on US winter, *Environ. Res. Lett.*, *8*; doi:10.1088/1748-9326/8/1/014019.

Yu, J.-Y., H.-Y. Kao, and T. Lee (2010), Subtropics-related interannual sea surface temperature variability in the equatorial central Pacific, *J. Climate*, *23*, 2869–2884; doi: http://dx.doi.org/10.1175/2010JCLI3171.1.

Yu, J.-Y., H.-Y. Kao, T. Lee, and S. T. Kim (2011), Subsurface ocean temperature indices for central-Pacific and eastern-Pacific types of El Niño and La Niña events, *Theor. App. Climatol.*; doi: 10.1007/s00704-010-0307-6.

Yu, J.-Y., F. Sun, and H.-Y. Kao (2009), Contributions of Indian Ocean and monsoon biases to the excessive biennial ENSO in CCSM3, *J. Climate*, *22*, 1850–1858.

Yu, J.-Y., H. Paek, E. S. Saltzman, and T. Lee (2015b), The early-1990s change in ENSO-PSA-SAM relationships and its impact on Southern Hemisphere climate, *J. Climate*; doi: 10.1175/JCLI-D-15-0335.1, in press.

Yu, J.-Y., M.-M. Lu, and S. T. Kim (2012a), A change in the relationship between tropical central Pacific SST variability and the extratropical atmosphere around 1990, *Environ. Res. Lett.*, *7*, 034025; doi:10.1088/1748-9326/7/3/034025.

Yu, J.-Y., Y. Zou, S. T. Kim, and T. Lee (2012b), The changing impact of El Niño on US winter temperatures, *Geophys. Res. Lett.*, *39*, L15702; doi:10.1029/2012GL052483.

Yu, J.-Y., P. -K. Kao, H. Paek, H. -H. Hsu, C. -W. Hung, M. -M. Lu, and S. -I. An (2015a), Linking emergence of the Central-Pacific El Niño to the Atlantic multi-decadal oscillation, *J. Climate*, *28*, 651–662; doi:10.1175/JCLI-D-14-00347.1.

Yu, W., B. Xiang, L. Liu, and N. Liu (2005), Understanding the origins of interannual thermocline variations in the tropical Indian Ocean, *Geophys. Res. Lett.*, *32*, L24706; doi:10.1029/2005GL024327.

Yuan, X. (2004), ENSO-related impacts on Antarctic sea ice: A synthesis of phenomenon and mechanisms, *Antarctic Sci.*, *16* (04), 415–425.

Yuan, X., and C. Li (2008), Climate modes in southern high latitudes and their impacts on Antarctic sea ice, *J. Geophys. Res*., *113*, C06S91; doi:10.1029/2006JC004067.

Yuan, X., and D. G. Martinson (2001), The Antarctic dipole and its predictability, *Geophys. Res. Lett.*, *28*, 3609–3612.

Yuan, Y., and S. Yang (2012), Impacts of different types of El Niño on East Asian climate: Focus on ENSO cycles, *J. Climate*, *25*, 7702–7722.

Yuan, Y., S. Yang, and Z. Zhang (2012), Different evolutions of the Philippine Sea anticyclone between eastern and central Pacific El Niño: Possible effect of Indian Ocean SST, *J. Climate*, *25*, 7867–7883.

Yulaeva, E., and J. M. Wallace (1994), The signature of ENSO in global temperature and precipitation fields derived from the microwave sounding unit, *J. Climate*, *7*, 1719–1736; doi:10.1175/1520-0442[1994] 007<1719:TSOEIG>2.0.CO;2.

Zebiak, S. E. (1989), Ocean heat content variability and El Niño cycles, *J. Phys. Oceanogr.*, *19*, 475–486; doi:10.1175/1520-0485%281989%29019<0475%3AOHCVAE>2.0.CO%3B2.

Zelle, H., G. J. van Oldenborgh, G. Burgers, and H. Dijkstra (2005), El Niño and greenhouse warming: Results from ensemble simulations with the NCAR CCSM, *J. Climate*, *18*, 4669–4683.

Zhang, L., L. Wu, X. Lin, and D. Wu (2010), Modes and mechanisms of sea surface temperature low-frequency variations over the coastal China Seas, *J. Geophys. Res.*, *115*, C08031; doi:10.1029/2009JC006025.

Zhang, R., and T. L. Delworth (2007), Impact of the Atlantic multidecadal oscillation on North Pacific climate variability, *Geophys. Res. Lett.*, *34*, L23708; doi:10.1029/2007GL031601.

Zhang, R., A. Sumi, and M. Kimoto (1999), A diagnostic study of the impact of El Nino on the precipitation in China, *Adv. Atmos. Sci.*, *16*, 229–241.

Zhang, W., F. Jin, J. Li, and H. Ren (2011), Contrasting impacts of two-type El Niño over the western north Pacific during boreal autumn, *J. Meteor. Soc. Japan.*, *89*, 563–569.

Zhang, X. B., J. Sheng, and A. Shabbar (1998), Modes of interannual and interdecadal variability of Pacific SST, *J. Climate*, *11*, 2556–2569.

Zhang, Y., J. M. Wallace, and D. S. Battisti (1997), ENSO-like interdecadal variability: 1900–93, *J. Climate*, *10*, 1004–1020.

Zhou, L.-T., C.-Y. Tam,W. Zhou, and J. C. L. Chan (2009), Influence of South China Sea SST and the ENSO on winter rainfall over South China, *Adv. Atmos. Sci.*, *27*, 832–844.

Zhou, S., A. J. Miller, J. Wang, J. K. Angell (2002), Downward-propagating temperature anomalies in the preconditioned polar stratosphere, *J. Climate*, *15*, 781–792.

Zhou, W., and J. C. L. Chan (2007), ENSO and the South China Sea summer monsoon onset, *Int. J. Climatol.*, *27*, 157–167.

Zhou W., X. Wang, T. J. Zhou, C. Y. Li, and J. C. L. Chan (2007), Interdecadal variability of the relationship between the East Asian winter monsoon and ENSO, *Meteor. Atmos. Phys.*, *98*, 283–293; doi: 10.1007/s00703-007-0263-6.

Zhou, Z. Q., S. P. Xie, X. T. Zheng, Q. Y. Liu, and H. Wang (2014), Global warming–induced changes in El Niño teleconnections over the North Pacific and North America, *J. Climate*, *27*, 9050–9064.

Zhu, Y., W. Wang, W. Zhou, and J. Ma (2011), Recent changes in the summer precipitation patterns in East China and the background circulation, *Climate Dyn.*, *36*, 1463–1473.

Zou, Y., J.-Y. Yu, T. Lee, M.-M. Lu, and S. T. Kim (2014), CMIP5 model simulations of the impacts of the two types of El Niño on US winter temperature, *J. Geophys. Res. Atmos.*, *119*, 3076–3092; doi:10.1002/2013JD021064.

Zubiaurre, I., and N. Calvo (2012), The El Niño–Southern Oscillation [ENSO] Modoki signal in the stratosphere, *J. Geophys. Res.*, *117*, D04104; doi:10.1029/2011JD016690.